CONTRACTOR REPORT

SAND93—7040
Unlimited Release
UC—721

MICROFICHE

Individual and Combined Effects of Chloride, Sulfate, and Magnesium Ions on Hydrated Portland-Cement Paste

Toy S. Poole, Lillian D. Wakeley, Cameron L. Young
Structures Laboratory
U.S. Army Corps of Engineers
Waterways Experiment Station
Vicksburg, MS 39180-6199

Prepared by Sandia National Laboratories Albuquerque, New Mexico 87185 and Livermore, California 94550 for the United States Department of Energy under Contract DE-AC04-94AL85000

Printed March 1994

V.P(various pagings)

Issued by Sandia National Laboratories, operated for the United States Department of Energy by Sandia Corporation.

Available to DOE and DOE contractors from
Office of Scientific and Technical Information
PO Box 62
Oak Ridge, TN 37831

Prices available from (615) 576-8401, FTS 626-8401

Available to the public from
National Technical Information Service
US Department of Commerce
5285 Port Royal Rd
Springfield, VA 22161

NTIS price codes
Printed copy: A04
Microfiche copy: A01

SAND93-7040
Unlimited Release
March 1994

Distribution
Category UC-721

Individual and Combined Effects of Chloride, Sulfate, and Magnesium Ions on Hydrated Portland-Cement Paste

Toy S. Poole, Lillian D. Wakeley,
and Cameron L. Young

Structures Laboratory
U.S. Army Corps of Engineers
Waterways Experiment Station
Vicksburg, MS 39180-6199

ABSTRACT

Ground water with a high concentration of magnesium ion is known to cause deterioration to portland cement concretes. A proposed mechanism for this deterioration process published previously involves an approximate 1:1 replacement of Ca ions by Mg ions in the crystalline phases of hydrated cement. The current study was undertaken to determine which ions, among magnesium, chloride, and sulfate, cause deterioration; whether their deleterious action is individual or interdependent; and to relate this mechanism of deterioration to the outlook for a 100-yr service life of concretes used in mass placements at the Waste Isolation Pilot Plant.

Loss of Ca ion by cement pastes was found to be strongly related to the concentration of Mg ion in simulated ground-water solutions in which the paste samples were aged. This was true of both salt-containing and conventional cement pastes. No other ion in the solutions exerted a strong effect on Ca loss. Mg ion did not accumulate in the chemically altered cement paste at the same rate that Ca was lost. Ca-ion loss was more than six times the Mg-ion gain. No crystalline Mg-bearing phases were detected in the deteriorated pastes.

Ca ion left first from calcium hydroxide in the pastes, depleting all calcium hydroxide by 60 days. Some calcium silicate hydrate remained even after 90 days in the solutions with the highest concentration of Mg ion, while the paste samples deteriorated noticeably. Softening of the samples occurred without complete destruction of calcium silicate hydrate, and with no apparent formation of magnesium silicate hydrate. The results indicated a mechanism that involves dissolution of Ca phases and transport of Ca ions to the surface of the sample, followed by formation of Mg-bearing phases at this reaction surface rather than directly by substitution within the microstructure of hydrated cement.

Given that calcium hydroxide and calcium silicate hydrate are the principal strength-giving phases of hydrated cement, this mechanism indicates the likelihood of significant loss of integrity of a concrete exposed to Mg-bearing ground water at the WIPP. The rate of deterioration ultimately will depend on Mg-ion concentration, the microstructure materials of the concrete exposed to that groundwater, and the availability of brine.

ACKNOWLEDGEMENT

This work was performed for Sandia National Laboratories (SNL) supported by the U.S. Department of Energy under contract DE-AC04-76DP00789. The performing agency was the Concrete Technology Division (CTD), Structures Laboratory (SL), U.S. Army Engineer Waterways Experiment Station (WES), under SNL Document Number AA 2030. Dr. Lillian D. Wakeley, WES, was Principal Investigator. Dr. Frank Hansen was Project Manager for SNL, in Department 6121, of which Dr. Joe Tillerson is Manager.

Laboratory studies and data analysis for this report were accomplished in the CTD, during April through December 1992. Dr. Steven J. Lambert, SNL, recommended components and proportions for exposure solutions. Mr. John Cook prepared the specimens, Ms. Cameron L. Young managed the experimental exposures and chemical analyses, Dr. Charles A. Weiss, Jr., performed the X-ray diffraction analyses. Dr. Toy S. Poole coordinated laboratory activities and analyzed the data. Dr. Poole and Dr. Lillian Wakeley prepared the report, with assistance from Ms. Young.

This project was completed at the WES under the general supervision of Mr. Bryant Mather, Director, SL; Mr. James T. Ballard, Assistant Director, SL; and Mr. Kenneth L. Saucier, Chief, CTD. Director of WES was Dr. Robert W. Whalin. Commander and Deputy Director was COL Leonard G. Hassell, EN.

CONTENTS

Figures

Tables

BACKGROUND

The Waste Isolation Pilot Plant (WIPP) is a research and development facility of the U.S. Department of Energy. Its purpose is to demonstrate safe disposal of radioactive wastes from U.S. Defense activities. For nearly 20 years, the U.S. Army Engineer Waterways Experiment Station (WES) has provided research support to Sandia National Laboratories (SNL) involving cement-based grouts and concretes proposed for use in the WIPP facility.

One of the objectives of this research support at WES in recent years has been to develop concrete for use in the WIPP at the proposed repository horizon, and determine experimentally whether it will be durable for the approximate 100-yr operating life of the facility. Ground waters at the WIPP facility horizon (656 m underground) and close above it include high concentrations of a variety of ions, some of which are known to cause deterioration and loss of strength in hardened concrete in many environments. Most notable of these ions in WIPP ground waters are magnesium, sulfate, and to a lesser degree, chloride (Lambert et al., 1992).

Previous Work at WES Showing Deterioration Associated with Magnesium Ions

In 1990, 5-yr-old concrete in the liner of the WIPP waste-handling shaft was found to have deteriorated. One major conclusion from these studies was that observed deterioration was related to high magnesium ion levels in the ground water (Wakeley et al., 1992; Lankard, 1990). Following this study, laboratory work was initiated at the WES to determine the extent to which some of the concrete mixtures and materials being considered for use at the WIPP were adversely affected by a simulated, worst-case, high-magnesium ion ground water. The simulated ground water used for that research was formulated by Lambert and designated H-1RSCM. Its composition was reported by Wakeley et al. (1992).

The results of the laboratory work had indicated that all of the mixtures under test were sensitive to H-1RSCM to varying degrees. The mechanism of deterioration was not identified because of the complex chemical compositions of both the brine and the cement-based mixtures chosen for study. Because the simulated ground water was highly concentrated in magnesium (Mg), sulfate, and chloride ions, it was difficult to tell which of these was causing most of the damage. The cementitious materials were mixtures of portland cement, with and without different fly ashes and

shrinkage-compensating components. These different cementitious or pozzolanic components gave each mixture a complex initial phase assemblage. The cement and fly ash each was a source of the hydrated phases with potential to react with Mg. The dolomitic aggregates also had been deteriorated, had lost strength, and could have contributed to the reaction products identified from this concrete.

While it was clear from the studies involving H-1RSCM that Mg ion was a factor in deterioration and loss of strength of these cementitious systems, it also was clear that studies of more simplified systems were more likely to reveal the mechanism of deterioration. It is important to know the mechanism, first so that the chemical threat to concrete performance, if any, is understood; and second, understanding of the mechanism is a tool to use in formulating materials systems with improved resistance to deterioration or identifying other necessary engineered barriers.

Hypotheses of the Deterioration Mechanism

Earlier conclusions about the effect of Mg on hardened cement paste, which is the strength-giving component of concrete, were derived from work on sulfate-attack problems and other forms of chemical deterioration of reinforced concrete in contact with sea water. Magnesium is a significant component of seawater, and its potential to initiate chemical changes to cement paste has been reported widely (Mather, 1966; Buck et al., 1984; Massazza, 1985; Bonen and Cohen, 1992).

There has been some research on the effects of other Mg salts (Biczok, 1972; Ftikos and Parissakis, 1985; Helmy et al., 1991; Kuenning, 1966; Oberst-Padtberg, 1985; Smolczyk, 1968), although this subject commonly has been a side issue to a study with some other focus. The deterioration mechanism for the action of magnesium has been proposed as a two-step process.

First, water containing magnesium ions penetrates into the hardened paste and precipitates as magnesium hydroxide (MH) when it encounters the high-pH pore fluid which is a saturated solution of calcium hydroxide (CH). Most of the calcium hydroxide exists in the solid state. Calcium (Ca) is solubilized from solid calcium hydroxide by a reaction between calcium hydroxide and magnesium ions and can diffuse out of the paste if a concentration gradient exists. The following reaction illustrates this process:

$$Ca(OH)_2[solid] \rightharpoonup Ca^{2+} + 2OH^{1-} + Mg^{2+}[solution] \rightharpoonup Mg(OH)_2 + Ca^{2+}$$

Since MH is very insoluble, its precipitation depletes OH^- from solution, causing more CH to dissolve to maintain the pore fluid in a saturated condition. Consequently, CH in the solid state can become severely depleted. MH occupies a larger volume than the CH it replaces, causing microfractures in the paste and allowing further entry of aggressive fluids.

The second step of the proposed mechanism continues as Mg enters an exchange reaction for the Ca in calcium silicate hydrate (CSH), eventually forming magnesium silicate hydrate (MSH), which is non-cementitious. The following reaction approximates the case of sea water, where the sulfate ion is important (Mather, 1966).

$$3CaO{\cdot}2SiO_2{\cdot}nH_2O + MgSO_4 \rightleftharpoons CaSO_4{\cdot}2H_2O + Mg(OH)_2 + SiO_2{\cdot}nH_2O$$

$$4Mg(OH)_2 + SiO_2{\cdot}nH_2O \rightharpoonup 4MgO{\cdot}SiO_2{\cdot}8.5H_2O + (n-4.5)\ H_2O$$

There may also be secondary effects due to the anions in the brine, which may not be covered by above reactions. Sulfate and chloride ions react with aluminates in the cement paste to form calcium sulfoaluminate and calcium chloroaluminate, respectively. Both of these compounds have the potential to be destructive, depending on how and when they form in the paste. These secondary effects could exacerbate the hypothesized primary effect of magnesium on calcium silicate hydrate.

This proposed two-step deterioration process, though plausible, was not confirmed by analyses of the reaction products from H-1RSCM brine and various cementitious solids. There was very little, if any, direct evidence that MSH or other magnesium-bearing compounds had formed in the deteriorated solids (Wakeley et al., 1992). And there was no compelling evidence that the sulfates in the simulated ground water were causing any serious degradation, although sulfate attack had been proposed as a deterioration mechanism for the WIPP waste-shaft-liner concrete (Lankard, 1991).

Purpose of the Research Reported Here

This work was undertaken to identity mechanisms of deterioration of cement paste caused by magnesium, chloride, and sulfate, and to determine whether the deleterious effects of these ions are

individual or interdependent. A further purpose was to relate mechanisms of deterioration to the likelihood that a mass concrete will serve as intended for the 100-yr operating life of the repository.

The presence of brines with abundant magnesium, sulfate and chloride in the Salado Formation creates a potentially difficult service environment for portland-cement concretes to be used as seal components. Concrete is the most practical material to use for large-scale load-bearing members of the seal system. If the concrete could be placed in brine-free regions of the repository, where no brine is present, the potential for chemical deterioration would be minimal. However, brines can migrate. Also, load-bearing members may be required in areas where brines are unavoidable. Therefore, the nature and likelihood of interactions between concrete and brine control the potential for acceptable service.

SELECTION OF MATERIALS AND SPECIMENS

The basis for selection of materials for the experimental matrix was twofold. First, materials used for fabricating specimens had to be related directly to the overall WIPP materials research program at the WES. The research on geochemical stability of cement-based seals needs to provide information useful to the research and development of candidate concretes. Therefore, it must involve materials that are realistic candidates for concrete components. For this reason, cements with no tricalcium aluminate (C_3A) were not considered because they are not readily available. Those with a high percentage of C_3A were omitted from consideration because of their susceptibility to several forms of chemical attack in this environment.

The second basis for selection of materials was the need to keep the system simple enough that reaction products could be related to reaction mechanisms between portland cement and brine components. Fly ash and shrinkage-compensating admixtures were omitted from the pastes in the experimental matrix, even though both materials are included in the current candidate concrete. This was to remove any question of the source of the reacted phases, by having only a single source (cement) for the hydrated phases susceptible to reaction with magnesium ions.

The Cement Selected

The cement selected was a Class H oilwell cement. The WES has a successful history of using this cement in grouts and concretes for underground containment systems (Gulick and Wakeley, 1989; Wakeley, 1990). It is a major cementitious component of the Salado Mass Concrete, the mass concrete formulation currently recommended by WES for WIPP panel seals (Appendix A).

Oilwell cement is basically a portland cement that has been chemically and physically formulated to allow extended working time under conditions of elevated temperature and pressure (Smith, 1990). The most obvious difference between oilwell cements and conventional portland cements is the relatively coarser particle size distribution of oilwell cements. Also, this particular cement was formulated to be resistant to chemical interaction with high levels of sulfate ion in its service environment. Chemical and physical properties of the cement are summarized in Appendix A.

Brine Solutions

Published work on concrete in seawater (references given p. 2) and WES experience indicate that magnesium, sulfate, and chloride have strong potential to initiate deterioration of hydrated cement phases in environments where concrete is in contact with waters containing dissolved salts. These were the ions of interest in the matrix of solutions.

Because of charge-balance constraints, concentrations of magnesium, sulfate, and chloride ions could not be varied in completely independent ways without introducing other ions. This would have required assumptions about the action of or interactions with the additional ions, which were precluded by the need for simplicity. Therefore, the solution matrix was selected to create wide but controlled variation within the constraints allowed by sodium and magnesium, present in the solutions initially as sulfate and chloride salts. The solution matrix was established by joint effort of SNL and WES researchers, with ion concentrations recommended by SNL.

All solutions in the matrix contained some concentration of each of the three ions of principal interest. This simulates reality in that ground waters in the vicinity of the WIPP contain some concentration of these ions. Brine compositions, based on analyses of waters from the Rustler Formation, are described in Table 1. Relative concentrations of each of the three major ions are designated as "H," representing the highest concentration expected in ground water; "M," representing moderate concentrations; and "L," representing the lowest concentration expected. The range of concentrations varied over two orders of magnitude. This was intended to reveal whether or not there is a threshold effect, that is, a concentration of Mg or other critical ion below which it is not a serious problem. Also, it was intended to reveal whether each ion presents a potential for chemical interaction with cement individually, or only in combination with one or more of the other critical ions.

Selection of Sample Size and Shape

Another goal of the experimental design was to use a specimen configuration that would cause most of the volume of each specimen to undergo the prevailing reactions in a manageable length of time without being artificially accelerated by heat or other means. In the previous work, we had used

Table 1. Composition of Solutions

		Ion			Salt			
Soln	Units	Cl	SO_4	Mg	NaCl	$NaSO_4$	$MgCl_2 \cdot 6 H_2O$	$MgSO_4 \cdot 7 H_2O$
1	Rel Conc[1]	H	H	H				
	g/L	200	20	50	113.67		375.80	51.34
	M[2]	5.63	0.21	2.06				
2	Rel Conc	H	L	H				
	g/L	200	0.2	50	89.57		417.72	0.51
	M	5.63	0.002	2.06				
3	Rel Conc	H	H	L				
	g/L	200	20	0.5	329.76	29.66		5.07
	M	5.63	0.21	0.02				
4	Rel Conc	M	M	M				
	g/L	20	2	5	11.37		37.58	5.13
	M	0.56	0.02	0.21				
5	Rel Conc	H	L	L				
	g/L	200	0.2	0.5	327.60		3.76	0.51
	M	5.63	0.002	0.02				
6	Rel Conc	L	H	L				
	g/L	2	20	0.5	3.30	26.66		5.07
	M	0.056	0.21	0.02				
7	Saturated $Ca(OH)_2$							
8	Deionized water							

[1] Relative concentration
[2] Molarity

2-in. cubes immersed in brine, which resulted in reaction gradients inward from the outside of each cube. This zoning caused complications in carrying out the post-treatment chemical analyses: from an analytical viewpoint, each zone was a separate sample. To avoid this diffusion-controlled zoning in the present study, relatively thin disc specimens of hardened paste were exposed to each solution. If deterioration was active, each specimen could be expected to undergo chemically controlled deterioration throughout its small thickness during a relatively short exposure time and at a temperature representative of the proposed repository.

Discs 3 mm thick were chosen to achieve the goal of total-volume reactivity. Samples thinner than this were not expected to have sufficient strength after the reactions to remain intact during handling, photography, and preparation for analysis. With this small sample size, however, we could not use compressive strength measurements to monitor the reactions by strength loss. Monitoring progress of reactions by presence of Mg-bearing phases also was not reasonable, given that such phases had not been positively identified as replacing cement paste. Results of the work involving 2-in. cubes had indicated that deteriorated zones always lost calcium (Wakeley et al., 1992). With total reaction of each sample in the present study, changes in the composition of discs could be monitored by X-ray diffraction (XRD) and by non-destructive bulk chemical analysis using energy-dispersive X-ray fluorescence (bulk XRF). Changes indicated by analyses of solids could be cross-checked by concomitant changes in brine composition, and phase composition of precipitates. Characteristics of cement-paste specimens are summarized in Table 2.

Table 2. Characteristics of Cement-Paste Specimens

Property	Description
Cement	Class H Oilwell Cement
Water-Cement Ratio, by mass	0.40
Mixing Water	a) saturated NaCl solution ("salt") b) deionized water ("non-salt")
Disc Diameter	20 mm
Disc Thickness	3.0 mm
Mass of typical disc	2.2 grams

Preparation of Specimens

Cement pastes were mixed according to ASTM C 305. Two types of pastes were prepared: 1) using deionized water for mixing, designated "non-salt"; and 2) made with mixing water saturated with sodium chloride, designated "salt." The salt-saturated condition is more meaningful to the overall project needs, given that the candidate Salado Mass Concrete is salt-saturated. The non-salt mixtures were included in the study because of anticipated questions about the effects on long-term durability of initial salt-saturation of concrete. Also, they were expected to contribute to understanding the mechanism of deterioration.

Pastes were cast in 20- by 70-mm plastic vials with snap caps, and were cured at 80° F (simulating field temperature) for 30 days in these vials. Selection of 30 days as the age of pastes when tests were initiated was arbitrary but reasonable. Given that properties of cement-based materials are time dependent, the age of the cement paste when specimens were first immersed in the test solutions could alter the rate of reactions, but not the fact that reactions occur. Exposing the samples to brines at a very early age -- i.e. during setting and soon after -- did not seem necessary for simulating field conditions. In panel seals or bulkheads, it is unlikely that brine will participate in initial hydration reactions. Brine movement at the proposed repository horizon is very slow (Krumhansl et al., 1991) and it is unlikely that a significant quantity of brine would arrive at the interface between concrete and host rock early enough to affect formation of initial hydration products. Thirty days was selected as a reasonable age by which concrete in a panel seal might be exposed to a significant quantity of ground water.

After the 30 days of curing in vials, paste cylinders were demolded and cut into 3-mm-thick discs with a diamond-bladed saw, using a light oil as a lubricant. Discs were cleaned with acetone to remove the oil, and allowed to air dry for 24 hours. Some pastes were left in the molds and later demolded and cut for analysis as control specimens.

Individual discs were randomly selected and each was immersed in one of the eight exposure solutions. Volume of solution was 30 mL, which was calculated to give a ratio of magnesium ion in solution to Ca ion in the paste of at least 10, for solutions having high (H) Mg concentration. This was intended to insure that lack of available magnesium did not become a reaction-limiting factor during the experiment.

METHODS OF ANALYSIS

Chemical and Compositional Analysis

Discs were removed from the solutions after 14, 30, 60, and 90 days of immersion. The discs removed after 14-day exposure were used for development of techniques of sample preparation and analytical methods. Consequently, data from this early age are not reported. Discs from most solutions were covered with a white precipitate, or crystalline growth, at all ages. Surface deposits are described in Appendix B. This surface coating was scraped off and saved for X-ray diffraction (XRD) analysis. Discs were then processed and analyzed for elemental composition by X-ray fluorescence (XRF), and for mineralogical composition by XRD, as described below. Compositions of residual brine solutions also were analyzed by XRF. The following paragraphs describe sample preparation and analyses.

Precipitates were removed from the surface of each disc with a razor blade. The remaining residue of precipitate was sanded off using 14.5-μm aluminum oxide powder. Each disc was then washed with methanol in an ultrasonic cleaner for about 30 seconds. After washing with acetone and drying in air, the disc was labeled and vacuum dried for 48 hours, to achieve constant mass and stop reactions.

For XRD analysis, a portion of each disc sample was ground to pass a 45-μm sieve and loaded into a sample holder as a random powder mount. Samples of surface precipitates were mounted as slurries. XRD patterns were collected from samples in air at room temperature, using a Philips APD 1700 system, operated from 2 to 70° 2θ using Cu radiation and a scan rate of 2° 2θ per minute.

For elemental analysis, the portion of the disc used for XRD was recovered and combined with the rest of the disc. These were ground to pass a 45-μm sieve and ignited at 900° C for 15 minutes. The sample was uniformly combined with boric acid (4:1), as a binder. Each sample was pressed into a pellet using an hydraulic press, to be analyzed using XRF. The backing of the pellet consisted of 4.0 g of boric acid.

These samples were analyzed on a Kevex energy dispersive X-ray fluorescence spectrometer using the Energy-dispersive X-ray Analysis Technique (EXACT). This procedure was developed by Harmon et al. (1978), as referenced by Kevex Instruments (1990), and is included as part of the

Kevex proprietary software, "Toolbox" (Kevex Instruments, 1990). The procedure combines the use of fundamental parameters with the known composition of a single standard. The standard was a sample of a disc that had not been exposed to any solution, and prepared as described above. The composition of this standard was determined as described in ASTM C 114, using atomic absorption, gravimetric, and volumetric techniques. By convention, elemental-analysis results are expressed as oxides.

Compositions of brine solutions also were analyzed by XRF. One mL of solution was placed in a plastic cup the bottom of which was a thin film of mylar. A small watch glass was placed over the cup to prevent evaporation. The system was flushed with helium. The EXACT procedure also was used for these analyses, with a brine solution of known composition as a standard. The composition of this standard solution is summarized in Appendix A. Solutions were analyzed at 14 through 60 days without modification. At 90 days, solutions were acidified with HCl, when it was apparent that the solutions were clouded with suspended solids. Heterogeneous samples such as these can cause bias in results, as discussed later (see Results).

Apparent Changes and Their Correction Factor

Comparison of oxide compositions among conditions from simple elemental analysis can result in misleading conclusions. As a result of exposure to salt-bearing solutions, some of the specimens either gained or lost chemical species, or both. This resulted in a net mass change. Because oxides are determined as percentages of the total mass, the relative amounts of some oxides would change as a result of mass loss or gain to the specimen, even if none of that particular oxide was gained or lost from the paste. For example, if NaCl enters a sample of paste during exposure to solution, but nothing leaves the paste, the analyzed composition of that paste will show a relative decrease in all of the other components. The apparent loss will be proportional to the mass increase associated with the NaCl. Therefore, the solid being analyzed would appear to have lost Ca, even though none actually left the system.

A direct way to compensate for this effect would be to measure mass changes of the specimens and to correct accordingly. This direct determination of mass change was not possible because of the precipitates that formed on the surfaces of each disc and the physical abrasion required to remove

them. Instead, we chose to use the apparent amount of a non-mobile oxide as a basis for a correction procedure, as described below.

Analysis of solution chemistry showed that neither SiO_2 nor Fe_2O_3 were lost from the pastes as a result of exposure to any of the solutions. This is consistent with other analyses of concretes exposed to natural brines. Therefore, it is reasonable to assume that changes in apparent composition of either of these oxides represents mass changes in the specimen, rather than any real gain or loss of Fe or Si. This became the basis of a correction factor, which then was applied to the other oxide compositions to identify real changes in percentages of other oxides.

The correction factor was calculated as the ratio of the value of the indicator oxide (either SiO_2 or Fe_2O_3) determined under control conditions, to the value after the experimental exposure. No mass changes could have occurred under control conditions because samples were sealed in plastic vials. A value less than unity indicates mass loss from the system. The following equation represents the correction,

$$A_c = A \cdot \left[\frac{B_{control}}{B_{exposed}} \right]$$

where A_c is the corrected value of the oxide in question, A is the value of that oxide obtained from a simple elemental analysis, $B_{control}$ is the value of SiO_2 or Fe_2O_3 of the control specimen, and $B_{exposed}$ is the value of SiO_2 or Fe_2O_3 after exposure to solution. Two different correction factors were calculated, one each based on SiO_2 and Fe_2O_3. The values compared favorably. Values for the SiO_2-based correction are in Table 4. Fe_2O_3-based correction factors are in Appendix C.

Statistical Considerations

Results from each experimental condition represent a single replicate, so it is not possible to calculate experimental error limits directly from results for each condition. Given that the experiments were intended to reveal time-dependent trends and not compare individual data points, this was not considered a problem. However, there are instances when this kind of direct comparison of single results from two different conditions is useful. In these instances, it is important to have an estimate of the size of the random error component of the experiment.

An estimate of experimental error can be obtained from the analysis of the controls. Both the salt and the non-salt control specimens were analyzed on 3 occasions. Because these controls were sealed in plastic vials, their composition was assumed to be constant and the three analyses are taken as independent replicates. Variation among these replicates gives an estimate of experimental error based on 4 degrees of freedom. These estimates, along with 95% confidence intervals associated with the single observation typical of the remainder of the data, are in Table 3.

Table 3. Estimates of Experimental Error Associated with Corrected Oxide Analysis

Analyte	Std. Dev. estimated from controls	95% Confidence Intervals, single observations
CaO	3.47	9.64
MgO	0.04	0.10
SiO_2	1.86	5.16
SO_4	0.13	0.37
Cl	0.76	2.11
Al_2O_3	0.09	0.25
Na_2O	0.90	2.49

If two values differ by more than the amount of the 95% confidence interval, then the difference is probably larger than would be attributable to random error. For example, the CaO level in paste specimens made with salt and exposed to solution 1 for 90 days was 37.29% (see observation 3, in Table 4). The CaO levels of a similar specimen exposed for 90 days to solution 3 was 30.45 (see observation 6, Table 4). Whereas both of the values are considerably below the initial CaO condition, the 6.85% difference between them is reasonably to be expected from random error, so these data cannot be taken as conclusive evidence of a difference in effects on the cement paste of solutions 1 and 2.

Table 4. Oxide Analysis (%) Corrected by the SiO_2-Ratio Method

OBS[1]	COND[2]	AGE	CaO	MgO	Fe_2O_3	SO_4	Cl	Al_2O_3	Na_2O	CF[3]
1	1S	30	45.90	1.45	3.44	2.77	9.82	3.34	4.30	0.868
2	1S	60	41.02	1.72	3.75	2.75	8.59	3.66	1.68	0.807
3	1S	90	37.29	1.86	3.74	3.14	10.20	3.65	4.00	0.758
4	2S	30	44.45	1.59	3.44	2.49	10.13	3.36	4.55	0.840
5	2S	60	38.71	2.68	3.88	2.16	8.25	3.67	1.72	0.784
6	2S	90	30.45	5.14	3.44	2.05	8.47	3.77	2.80	0.675
7	3S	30	57.41	1.28	3.48	3.69	7.63	3.28	5.96	0.998
8	3S	60	57.51	1.34	3.69	3.35	7.38	3.46	5.71	0.998
9	3S	90	54.50	1.26	3.34	3.72	7.11	3.47	5.41	0.933
10	4S	30	43.84	1.25	3.17	4.10	2.99	3.26	0.65	0.761
11	4S	60	45.45	1.32	3.43	3.56	2.06	3.43	0.33	0.777
12	4S	90	41.78	1.26	3.16	3.94	3.94	3.53	0.31	0.714
13	5S	30	54.78	1.23	3.25	1.36	6.91	3.23	2.64	0.928
14	5S	60	56.50	1.21	3.66	0.88	6.80	3.43	2.62	0.983
15	5S	90	52.37	1.14	3.13	0.95	6.80	3.40	2.54	0.880
16	6S	30	53.21	1.20	3.18	6.37	1.01	3.13	0.81	0.893
17	6S	60	55.24	1.24	3.46	6.61	0.63	3.29	0.72	0.933
18	6S	90	51.19	1.20	3.14	7.05	0.59	3.32	1.20	0.836
19	7S	30	53.42	1.16	3.00	2.04	1.40	3.17	0.45	0.848
20	7S	60	54.75	1.20	3.22	1.95	1.15	3.33	0.13	0.876
21	7S	90	52.51	1.13	3.06	2.10	0.98	3.43	0.10	0.822
22	8 S	30	56.44	1.20	3.36	2.08	1.51	3.21	0.36	0.910
23	8 S	60	54.05	1.21	3.27	1.96	1.15	3.33	0.13	0.872
24	8 S	90	48.49	1.19	2.84	2.07	1.12	3.46	0.25	0.752
25	CS	30	53.06	1.24	3.24	2.17	7.17	3.32	4.66	0.947
26	CS	60	58.60	1.31	3.54	2.19	7.89	3.43	5.06	1.032
27	CS	90	58.27	1.26	3.41	2.45	9.23	3.39	7.02	1.026

(Continued)

[1] Observation numbers from statistical-analysis software for reference to specific results.
[2] Exposure condition, solution number from Table 1, salt (S) or non-salt (N).
[3] CF = Mass correction factor based on uncorrected SiO_2 values, Appendix C.

Table 4. (Concluded)

OBS[1]	COND[2]	AGE	CaO	MgO	Fe_2O_3	SO_4	Cl	Al_2O_3	Na_2O	CF[3]
1	1N	30	51.30	1.66	3.83	3.73	8.60	3.97	2.57	0.943
2	1N	60	49.10	2.29	4.09	3.99	9.10	4.16	1.85	0.926
3	1N	90	42.67	2.89	3.98	4.00	10.19	4.25	3.89	0.865
4	2N	30	54.44	2.10	4.03	3.22	8.22	4.31	2.33	0.983
5	2N	60	46.14	1.94	3.86	2.92	7.95	4.07	2.19	0.887
6	2N	90	39.63	2.46	3.55	2.87	8.01	4.19	1.63	0.785
7	3N	30	66.14	1.49	3.96	4.36	6.95	3.88	4.97	1.131
8	3N	60	66.01	1.61	3.94	5.05	6.78	4.05	4.75	1.125
9	3N	90	60.95	1.49	3.60	4.72	5.42	4.09	3.83	1.021
10	4N	30	50.35	1.55	4.04	4.48	2.17	4.04	0.42	0.873
11	4N	60	53.37	1.52	3.93	4.60	2.21	4.00	0.41	0.935
12	4N	90	47.06	1.46	3.63	4.62	1.48	4.17	0.30	0.806
13	5N	30	63.42	1.49	3.82	2.54	7.39	3.91	4.57	1.095
14	5N	60	63.31	1.49	3.81	2.28	6.80	3.93	2.98	1.095
15	5N	90	62.16	1.36	3.79	2.18	6.75	3.95	3.50	1.036
16	6N	30	63.30	1.61	3.68	6.15	0.36	3.88	0.44	1.036
17	6N	60	64.96	1.56	3.94	8.14	0.86	3.95	0.85	1.101
18	6N	90	60.16	1.42	3.54	8.79	0.24	4.08	0.55	0.978
19	7N	30	58.62	1.47	3.42	2.69	0.64	3.90	0.15	0.952
20	7N	60	62.49	1.53	3.67	2.58	0.19	4.17	0.17	1.006
21	7N	90	58.23	1.40	3.44	2.50	0.05	4.09	0.10	0.935
22	8N	30	61.73	1.46	3.61	2.65	0.06	3.92	0.11	0.969
23	8N	60	59.73	1.44	3.50	2.73	0.19	3.81	0.24	0.960
24	8N	90	55.50	1.40	3.29	2.44	0.04	4.14	0.16	0.873
25	CN	30	61.98	1.44	3.63	2.51	0.07	3.93	0.26	1.006
26	CN	60	66.61	1.47	3.83	2.70	0.43	3.93	0.54	1.068
27	CN	90	59.07	1.40	3.37	2.56	0.05	4.13	0.31	0.935

See footnotes on previous page.

RESULTS

Composition of Discs

Data from oxide analyses of discs are in Table 4. Samples and exposure conditions are summarized in a notation used in this and other tables. For example, "02N" means the specimen was exposed to solution 2 and was made with mixing water containing no salt. "S" indicates salt in the mixing water. "C" indicates control specimens, not exposed to solutions. Sometimes this notation is followed by another number, which indicates the time of exposure. For example, "08S60" means the specimen was made with salt in the mixing water, exposed to solution 8 for 60 days.

Data in Table 4 have been corrected by reference to SiO_2 values, as described previously. Both the SiO_2 and the Fe_2O_3 correction procedures revealed essentially the same patterns of chemical changes in the discs. The SiO_2-based correction appeared to be a little more conservative in its description of effects. Data plotted in the figures will be based on them, although general trends do not differ with the correction used. Results of the primary bulk analysis of the discs along with the corrected values obtained with the Fe_2O_3-based corrections are in Appendix C.

Table 5 summarizes the phases that were detected by X-ray diffraction (XRD) in the pastes after 14, 30, and 60 days exposure to brines. XRD data were not available for samples after 90-day exposure, due to inadvertent ignition of the specimens before XRD analyses were performed. In Table 5, the symbol (↓) for data from analyses after 30-day exposure indicates a decreased amount of this phase compared to the amount indicated by the 14-day analysis of the same sample. In addition to the phases described in Table 5, all samples have perceptible amounts of dicalcium silicate (C_2S) and tricalcium silicate (C_3S), representing unhydrated cement; and calcium silicate hydrate (CSH). Amounts of these phases remained fairly constant from 14 through 60-days exposure.

Calcium Phases

The most conspicuous brine-induced changes in the paste samples, detectable by elemental analysis, were in CaO levels. Large amounts of CaO were lost from specimens exposed to solutions highly concentrated in Mg ion (solutions 1 & 2). This effect is illustrated in Figures 1 and 2. The

Table 5. Crystalline Phases Detected by X-ray Diffraction in Pastes after Exposure to Solution

Sample	14 Days	30 Days	60 Days
Salt Control	CH, NaCl, CCA	CH, NaCl, CCA	CH, NaCl, CCA
01S	CH, Gypsum, NaCl, CCA	CH ↓, Gypsum, NaCl, CCA	Gypsum, NaCl, CCA
02S	CH, C_4AF, NaCl, CCA	CH ↓, NaCl, CCA	NaCl, CCA
03S	CH, NaCl, CCA	CH, NaCl, CCA	CH, NaCl, CCA, C_4AF
04S	CH, Ettringite	CH ↓, Ettringite	CH, Ettringite
05S	CH, NaCl	CH, NaCl, CCA	CH, NaCl, CCA, C_4AF
06S	CH, Gypsum	CH, Ettringite, Gypsum	CH, Ettringite, Gypsum, C_4AF
07S	CH	CH	CH, Ettringite
08S	CH, Ettringite	CH, C_4AF	CH
No Salt Control	CH, Ettringite	CH, Ettringite	CH, Ettringite
01N	CH, Ettringite, Gypsum	CH ↓	Ettringite, CCA
02N	CH, Ettringite, CCA	CH ↓, CCA	Ettringite, CCA
03N	CH, NaCl, Ettringite	CH, NaCl, Ettringite	CH, NaCl, Ettringite
04N	CH, Ettringite	CH ↓, Ettringite	CH, Ettringite
05N	CH, NaCl	CH, NaCl	CH, NaCl, Ettringite
06N	CH, Ettringite, Gypsum	CH, Ettringite, Gypsum	CH, Ettringite, Gypsum
07N	CH, Ettringite, C_4AF	CH, Ettringite, C_4AF	CH, Ettringite, C_4AF
08N	CH, Ettringite	CH, Ettringite	CH, Ettringite

In addition all samples have perceptible amounts of C_2S, C_3S, and CSH. The symbol (↓) indicates a decreasing amount of this phase compared to the earlier X-ray pattern of the same sample.

CH = calcium hydroxide
CCA = tetracalcium aluminate dichloride-10-hydrate
C_4AF = tetracalcium aluminoferrite
C_2S = dicalcium silicate
C_3S = tricalcium silicate
CSH = calcium silicate hydrate
Ettringite = 6-calcium aluminate trisulfate-32-hydrate

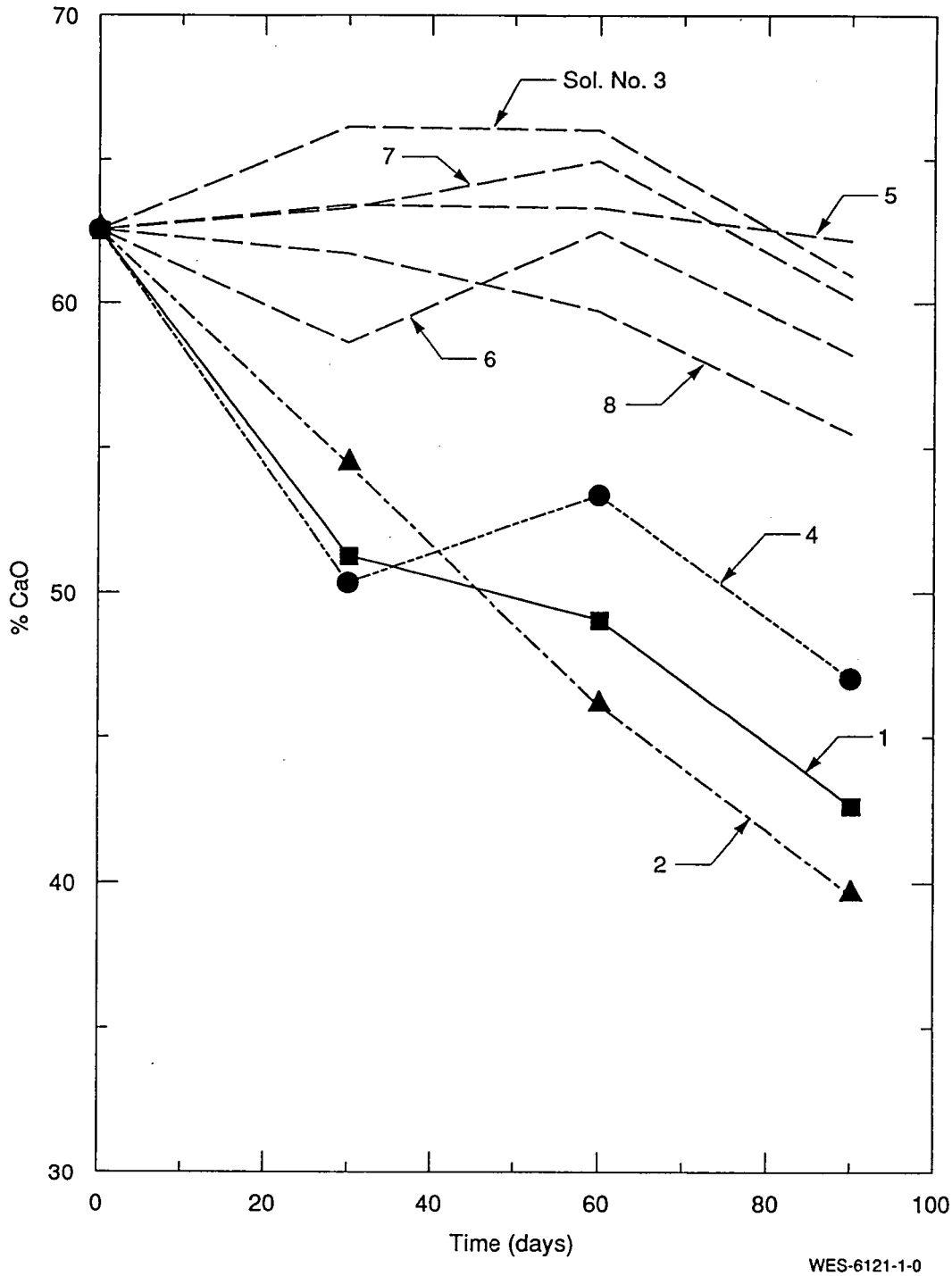

Figure 1. Percentage of CaO remaining in non-salt paste specimens.

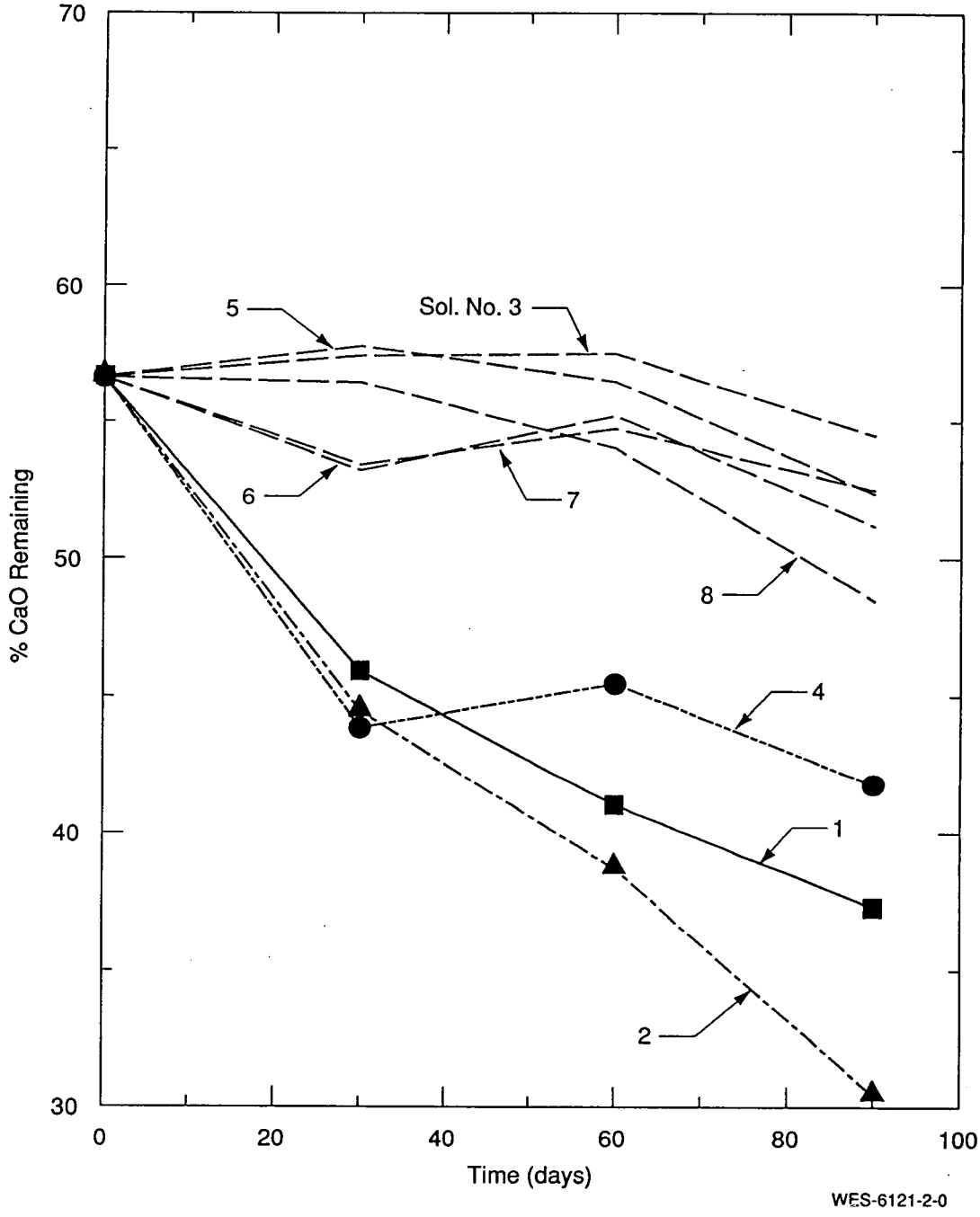

Figure 2. Percentage of CaO remaining in salt paste specimens.

loss rate appears to be relatively linear, particularly in the case of solution 2, and continuous through 90 days. Linear regression analysis of these data are presented in Table 6. Loss rates ranged from 0.21 to 0.28% per day. The presence of salt in the mixing water did not appear to exacerbate the CaO-loss rate, although this cannot be concluded definitively without more replication, which is underway.

Table 6. Loss Rates of CaO Estimated from Linear Regression

Exposure Condition	Salt/ Non-salt	Loss Rate (% per day)	90% Confidence Interval on Rate
1	N	0.21	0.12
2	N	0.27	0.03
4	N	0.14	0.19
8	N	0.08	0.05
1	S	0.21	0.11
2	S	0.28	0.09
4	S	0.14	0.20
8	S	0.08	0.06

The phase analysis indicated several changes in calcium phases that resulted from exposure to these two solutions. Calcium hydroxide decreased with time and was no longer detectable after 60 days exposure to these solutions, both in salt and non-salt pastes. Levels of CSH appear to be constant with time. Some calcium chloroaluminate, calcium sulfoaluminate, and calcium sulfate were detected in pastes, but their presence appeared to depend on the concentrations of sulfate and chloride ions in the solutions and did not appear to be related to magnesium levels. Therefore, these will be discussed below with sulfate and chloride compounds.

Detectable, but smaller amounts of CaO were lost from specimens exposed to the solution with a moderate Mg concentration (soln. 4), as illustrated in Figure 1. These data fit a linear model poorly. The CaO loss under this condition was considerable between 0 and 30 days exposure. Losses after 30 days were minor. Phase analysis indicated that CH was depleted between 14 and 30 days, but then persisted past 60 days.

Very small amounts of CaO were lost when specimens were exposed to deionized water. Loss rates were 0.08% per day (Table 6). At the level of detection allowed by this experiment, there was no CaO lost as a result of exposure to any of the other solutions.

There was some evidence that the CaO-loss effect in high-magnesium ion solution was influenced by the sulfate concentration of the solutions. As illustrated in Figures 1 and 2, specimens exposed to solution 1 (high Mg and SO_4) lost less CaO at later ages than did specimens exposed to solution 2 (high Mg, low SO_4). This difference was small relative to the experimental error estimated for single observations, but the nearly exact duplication of the pattern in both the salt and non-salt pastes may be significant.

Magnesium Phases

Patterns of magnesium accumulation in specimens are illustrated in Figures 3 and 4. Increases in MgO content of the specimens occurred in exposure to the two solutions with high Mg ion concentrations (solutions 1 and 2). The effect was small but detectable (outside estimated experimental error) relative to controls at 30 days, and accumulation continued through the 90-day test age. There was no detectable accumulation as a result of exposure to solution 4, which contained moderate levels of Mg ion.

Particularly conspicuous was the accumulation of MgO in salt-containing specimens exposed to solution 2, which was high in magnesium and chloride, but low in sulfate. No magnesium phases were detected in any of the disks by XRD analysis.

Silicon Phases

Changes in SiO_2 evidenced by elemental analysis are believed to be due solely to relative enrichment or depletion due to ingress or egress of other phases. When data were corrected by reference to Fe_2O_3, all SiO_2 values fell within the experimental error defined by controls (see Appendix B for these data). This conclusion was also supported by the data from analyses of post-test solutions, presented later.

Silicon phases were detectable by XRD only as hydrated or unhydrated calcium silicates in the pastes. Levels of these did not change perceptibly during the experiment.

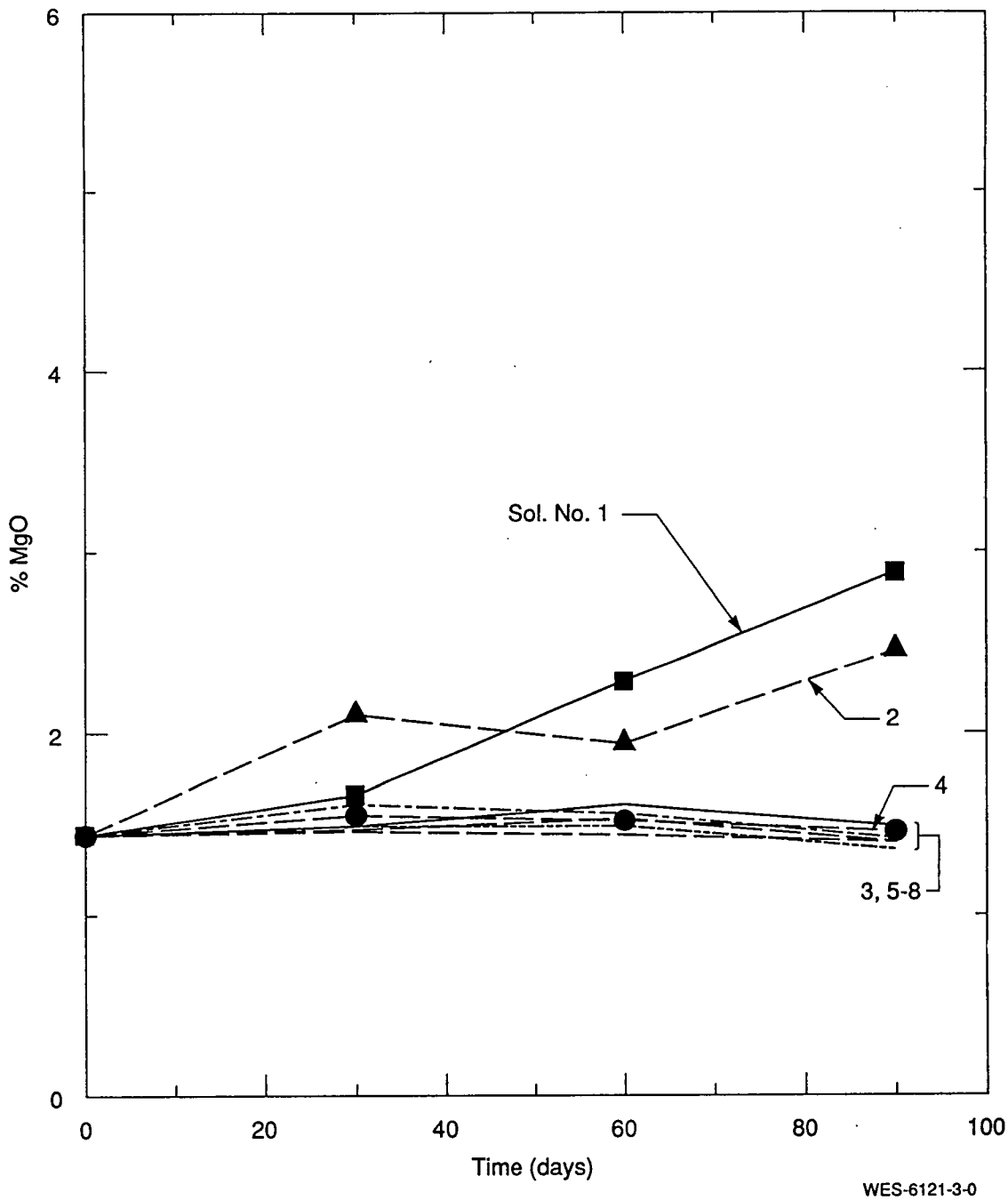

Figure 3. Percentage of MgO accumulated in non-salt specimens vs. exposure time.

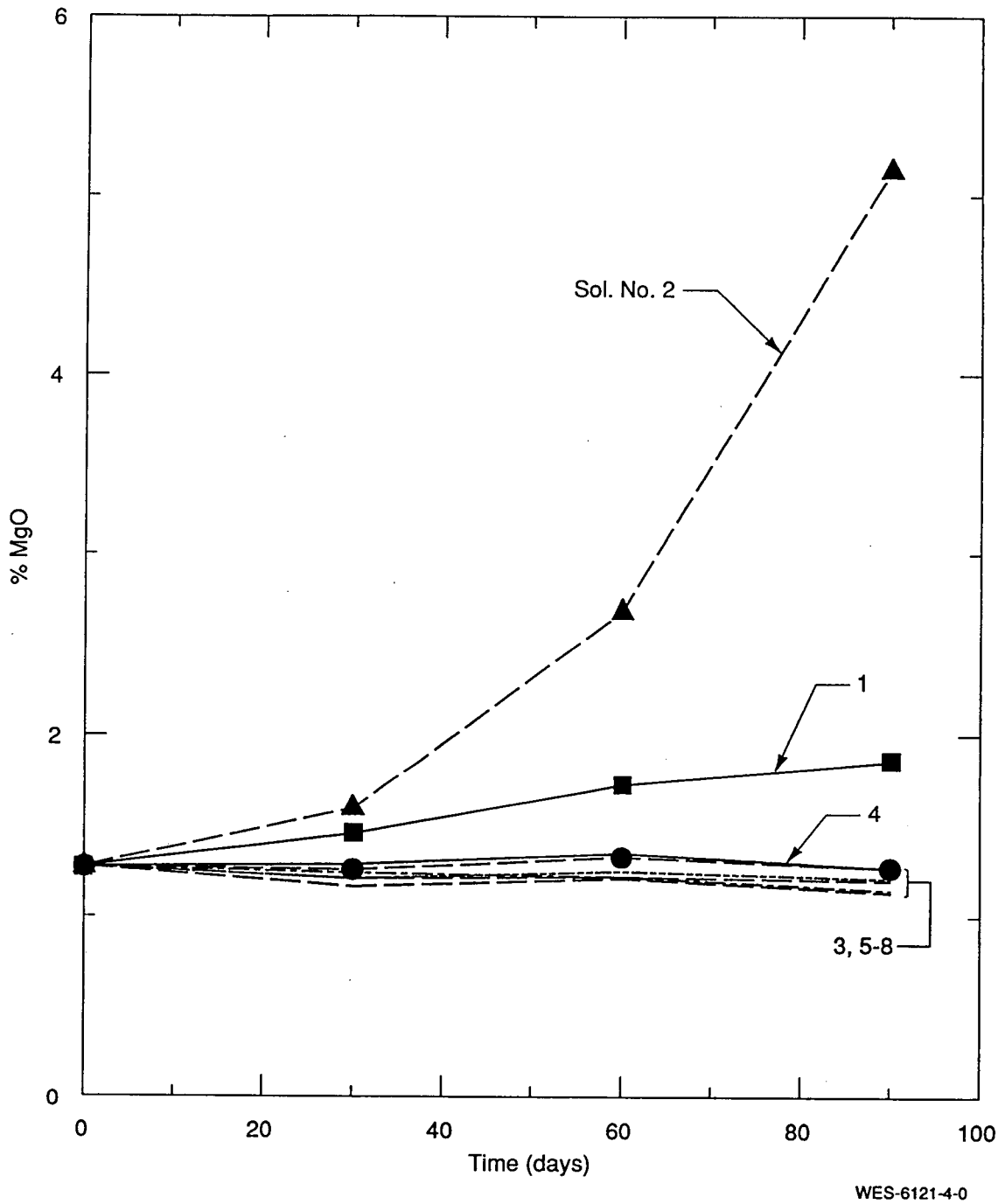

Figure 4. Percentage of MgO accumulated in salt pastes vs. exposure time.

Aluminum Phases

The aluminum content of the cement was low for a portland cement, so formation of major quantities of aluminum-based phases was not expected. Elemental analysis showed no changes in paste concentrations of Al_2O_3 as a result of exposure to any of the solutions. Results of XRD analysis indicated that the aluminum was active in formation of calcium sulfoaluminate and calcium chloroaluminate. These appeared to be controlled by the concentrations of chlorides and sulfates in solution, and therefore, will be discussed below.

Iron Phases

There was no evidence, from either XRF or XRD analyses, that iron played any active role in the reaction between hydrated cement paste and exposure solutions. Tetracalcium aluminoferrite (C_4AF), known to be a persistent phase in portland cement pastes, was detected after 60 days exposure of both non-salt and salt specimens to all solutions except for high-magnesium ion solutions. Although its presence was not always noted in XRD patterns, it does not come and go at random. Its presence is easily masked by other phases in complex assemblages.

Sulfur Phases

Sulfate ion appeared to be relatively mobile and reactive in this system. Concentrations appeared to be stable with time, reaching approximate equilibrium by 30 days. Figure 5 illustrates comparative accumulations among conditions at 90 days. Sulfate accumulations were high in specimens exposed to high or moderate sulfate ion concentrations in solution (solutions 1, 3, 4, and 6). Concentrations were particularly high in specimens exposed to solution 6, which was characterized by low chloride, high sulfate ion concentrations. Within these patterns, sulfate contents of non-salt specimens were always higher than those of salted specimens.

Gypsum and calcium sulfoaluminate (CSA) were the principal sulfate-containing compounds formed, as determined by XRD. In salt-containing specimens, CSA formed only when exposure was to solutions with low or moderate levels of chloride ion. In high-chloride high-sulfate ion solutions,

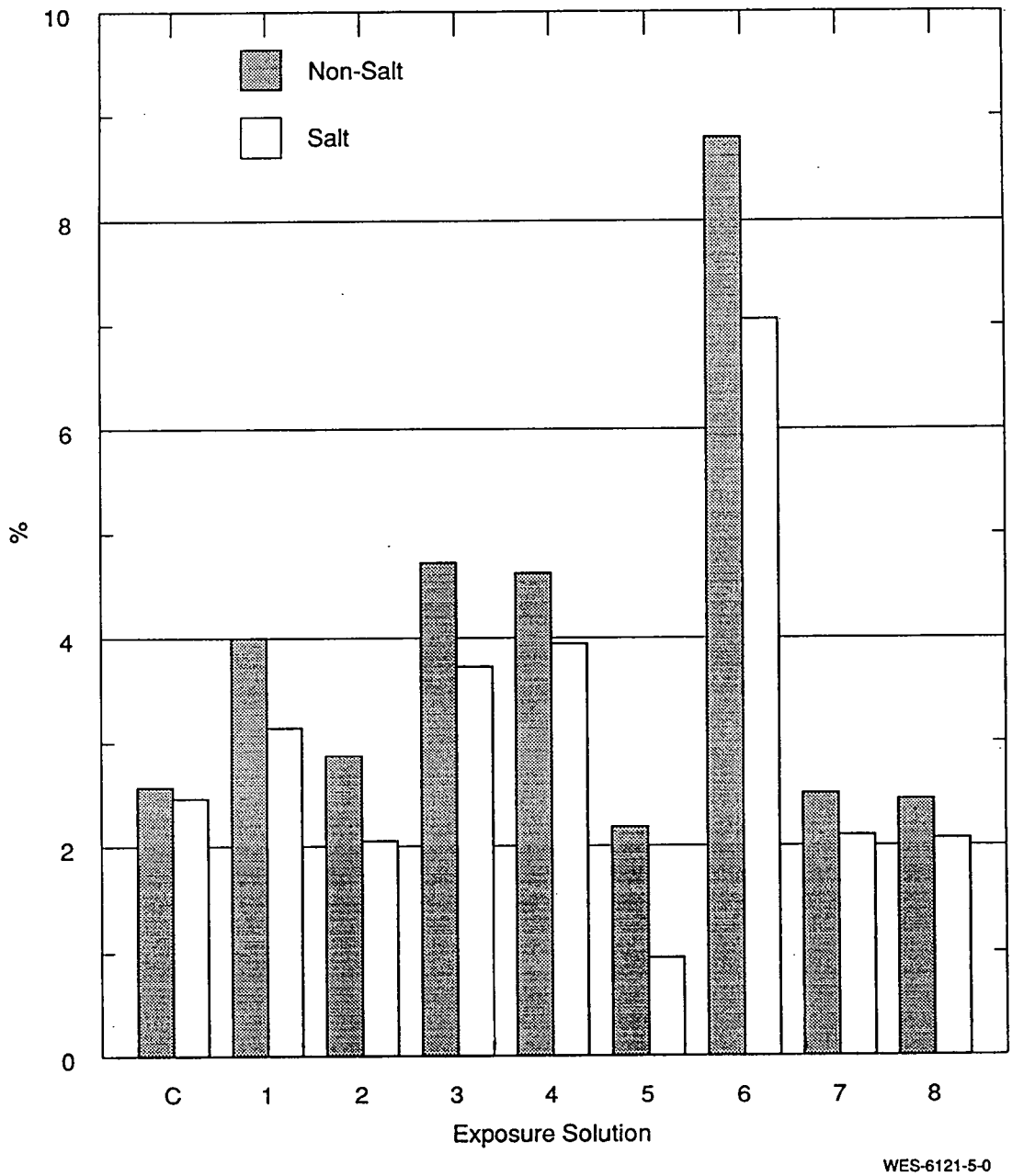

Figure 5. Accumulation of sulfate in cement pastes after 90 days in solutions.

gypsum was the principal sulfate-bearing phase. In non-salt specimens, CSA was the principal sulfate-bearing phase. Gypsum formed from exposure to solution 6 (low chloride, high sulfate ion).

Chlorine Phases

Chloride ion also appeared to be relatively mobile and reactive. Concentrations were essentially stable by 30 days. Figure 6 illustrates 90-day patterns of Cl-ion concentrations.

In salt-containing specimens, Cl-ion concentrations were high initially and stayed at similarly high levels when exposure was to high-Cl-ion solutions. Principal compounds identified by XRD were NaCl and calcium chloroaluminate (CCA). When exposed to low-Cl-ion solutions, concentrations of chloride in the specimens decreased to very low values, and these compounds ceased to be detectable by XRD analysis.

In non-salt specimens, Cl-ion concentrations were very low initially but approached levels comparable to the salt-containing specimens when the Cl ion concentration in the solutions was high. Somewhat less accumulation occurred in exposure to moderate chloride levels (solution 4). Except in exposure to solution 2, which was characterized by low sulfate concentrations, the principal Cl-containing phase detected by XRD was NaCl. No CCA was observed except in discs stored in solution 2.

Sodium Phases

Na_2O largely followed the pattern exhibited by chloride, except that where magnesium concentrations were high, Na_2O concentrations were somewhat lower. This generally reflects the composition of the brines. Brines with high magnesium concentrations contained less Na ion than brines with low Mg ion concentrations. This inconsistency in sodium concentration among solutions was necessary to maintain charge balance in the solutions. One exception to this pattern appears in a comparison of specimens made with salt exposed to solutions 3 and 5. Sodium levels in specimens exposed to solution 3 remain at about 5.5%, while those in specimens exposed to solution 5 drop to about 2.5%. The major difference in these solutions is that solution 3 contains high levels of sulfate.

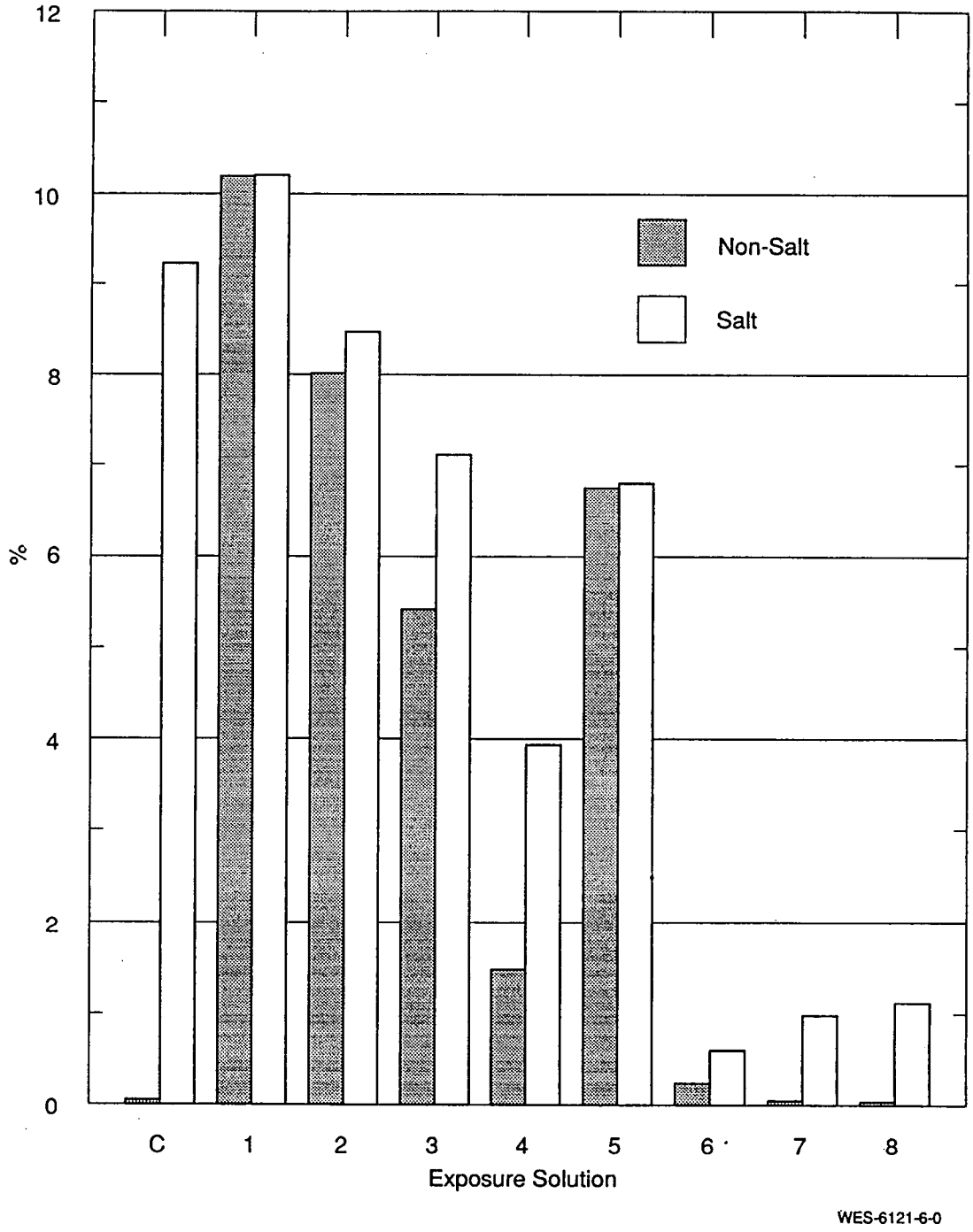

Figure 6. Total chloride in cement pastes after 90 days in solutions.

In general, sodium levels do not change much with time over the 30 to 90 day interval represented in these experiments. This suggests that whether or not salt was added to the cement paste, the sodium probably reaches equilibrium in the system by about 30 days.

Phase Composition of Precipitates

Precipitates from the surfaces of four discs with the largest amount of surface accumulation were examined by XRD after 60 days in solution (first four entries, Table 7). All precipitates were analyzed after 90 days (Table 7). The relative amount of each phase was estimated from peak heights in diffraction patterns. Peak height, of course, does not indicate abundance directly, and we did not perform quantitative XRD analyses.

Working definitions of the abundance terms from Table 7 are as follows:

Major: >30% of total sample

Minor: <30% and >5% of total sample, and

Trace: <5% of total sample.

The percentages given are approximations from experience with XRD data, and were not calculated. These terms indicate relative amounts of the principal phases that crystallized on disc surfaces during exposure to solutions, and do not indicate total amount of precipitate that formed. Removal of these precipitates for analyses was difficult because the pastes had softened.

The amount of material precipitated on disc surfaces depended on the concentration of magnesium ion in solution. Specimens exposed to solutions 1, 2, and 4, which were either high or moderate in magnesium ion concentration, were coated with substantial amounts of precipitate. Precipitates on specimens exposed to solutions with high concentrations of chloride or sulfate ion or both, but low magnesium ion, were light. There was no perceptible precipitate on specimens exposed to solutions 7 and 8 (lime water and deionized water, respectively). Figures 7 and 8 show precipitates on two specimens immediately after removal from solution. The precipitate shown in Figure 7 is typical of exposure to solutions high in Mg and SO_4 ions. Figure 8 illustrates typical precipitates formed after exposure to solutions high in Mg, but low in SO_4 ions. Descriptions of all precipitates are in Appendix B.

Table 7. XRD Analysis of Surface Precipitates after 60 and 90 Days in Solution						
	Phase					
Sample	$CaSO_4 \cdot 2H_2O$ Gypsum	$Mg(OH)_2$ Brucite	NaCl Halite	$CaCO_3$ Calcite	$C_6AS_3H_{32}$ Ettringite	$Ca(OH)_2$ Portlandite
01S60	Major	Minor	Minor			
02S60		Major	Minor	Minor		
04S60		Major	Minor	Minor		
01N60	Major	Minor	Minor			
01S90	Major	Major				
02S90		Major				
03S90	Major					
04S90		Major		Trace		
05S90				Trace		Major
06S90	Major					
07S90				Minor		Major
08S90				Minor	Trace	Major
01N90	Major	Major	Minor			
02N90		Major				
03N90	Major		Trace			
04N90		Major		Trace		
05N90			Minor	Minor		Major
06N90	Major	Minor				
07N90				Trace		Major
08N90	No detectable precipitates					

Figure 7. Photograph of specimen exposed to solution 1 for 90 days.

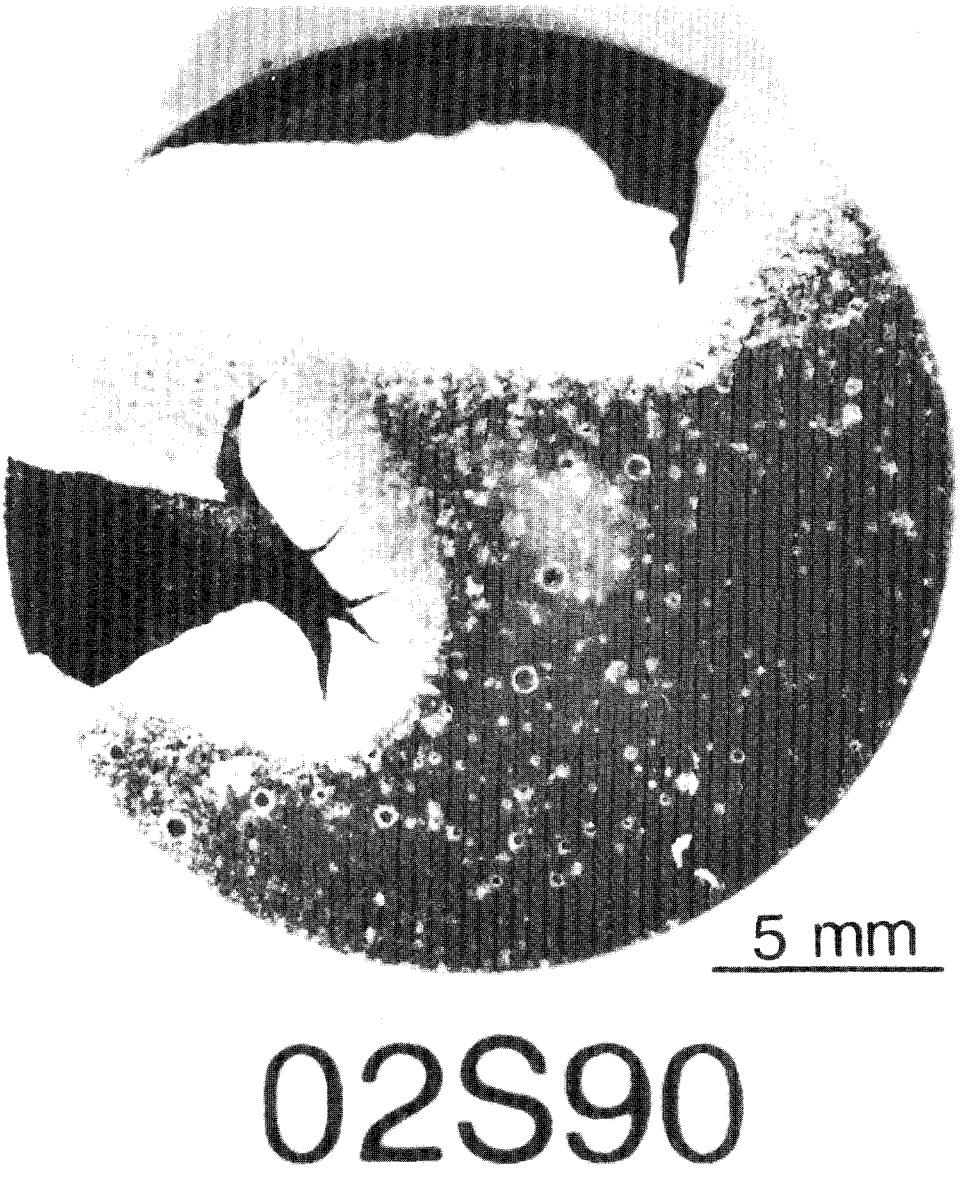

Figure 8. Photograph of specimen exposed to solution 2 for 90 days.

The composition of surface precipitates appeared to depend on the ions in solution and their concentrations. With the exception of some halite, all were calcium-based phases. $CaSO_4 \cdot 2H_2O$ (gypsum) was the major compound found in surface precipitates after exposure to high-sulfate solutions. $Mg(OH)_2$ (brucite) was the major compound found when exposed to high- or moderate-magnesium solutions. Both brucite and gypsum formed when both sulfate and magnesium were in high concentration in solution. $Ca(OH)_2$ (portlandite) was found on the surface of specimens exposed to solutions 5, 7, and 8. These discs showed either minimal or virtually no surface accumulation, so the CH could have been derived from inadvertent removal of paste when surfaces were scraped.

Composition of Liquid Phase

Data from post-exposure analyses of solutions are summarized in Table 8. These analyses were conducted principally to determine whether or not cement constituents were being removed from the hydrated cement paste as a result of exposure to the solutions. Liquid-phase analysis is particularly useful in detecting leaching of relatively small quantities of calcium-bearing cement compounds since there is no background level of these in the liquid phase to complicate the analysis. In addition, these analyses were used to verify that magnesium ion levels in solution were not depleted, either by reaction with cement paste or precipitation on the specimen surface, to the point of inhibiting potential degradation reactions. In principle, analysis of the liquid phase, along with analysis of precipitated material and paste, should give the opportunity for mass-balance analysis among these three phases. In practice, this is difficult because of the analytical errors. The biggest problem is in estimating the fraction of material in the surface precipitate phases. It is difficult to remove all of this material without also taking some of the disks. And there is suspended material as well. Unlike using liquid-phase analysis for detecting loss of cement compounds, using liquid phase analysis to estimate the concentrations of magnesium or other elements taken into the paste from solution is difficult. Because there are large quantities of these elements in the solutions, and because the ratio of liquid to specimen mass is large, relatively small changes in solution concentration occur, and these are close to the analytical error.

Table 8. Solution Chemistry after Exposure to Specimens

OBS	COND	AGE	Ca[1]	Mg[1]	Fe[2]	S[1]	Cl[1]	Al[2]	Na[1]
1	1N	0	0.00	17.13	868	2.32	53.91	464	14.26
2	1N	14	0.54	.	.	.	.	.	.
3	1N	30	0.41	17.56	37	1.16	51.43	561	12.61
4	1N	60	0.94	14.55	68	1.55	52.28	555	13.41
5	1N	90	0.85	13.79	25	0.90	51.95	472	13.60
6	2N	0	0.01	12.69	1500	0.55	52.54	370	8.56
7	2N	14	0.86	.	.	.	.	.	.
8	2N	30	1.26	14.97	709	0.56	51.21	656	10.74
9	2N	60	1.84	14.60	572	0.74	50.96	502	9.74
10	2N	90	2.05	14.00	135	0.80	52.34	474	10.89
11	3N	0	0.00	2.30	52	2.39	65.47	796	43.65
12	3N	14	0.43	.	.	.	.	.	.
13	3N	30	0.26	4.49	65	1.87	61.01	117	33.00
14	3N	60	1.10	9.95	60	2.12	62.10	482	39.10
15	3N	90	0.10	0.38	30	2.14	61.36	266	33.72
16	4N	0	0.00	3.20	556	0.99	9.52	365	2.86
17	4N	14	1.69	.	.	.	.	.	.
18	4N	30	3.16	0.30	228	0.37	7.70	199	0.68
19	4N	60	4.06	0.09	130	0.37	7.00	218	0.00
20	4N	90	1.71	0.91	58	0.59	8.73	307	1.75
21	5N	0	0.00	0.53	42	0.88	66.10	377	36.13
22	5N	14	0.37	.	.	.	.	.	.
23	5N	30	0.40	12.17	47	0.78	63.09	802	29.27
24	5N	60	0.64	12.16	54	0.79	62.78	559	30.37
25	5N	90	0.14	0.48	45	0.85	63.22	331	33.17
26	6N	0	0.01	1.10	52	5.85	2.30	664	4.15
27	6N	14	0.47	.	.	.	.	.	.
28	6N	30	0.31	3.02	82	3.95	2.00	425	3.86
29	6N	60	1.04	3.65	67	3.94	1.86	418	3.76
30	6N	90	0.28	0.73	48	3.29	6.52	289	3.74
31	7N	0	0.09	0.63	78	0.91	0.01	814	0.29
32	7N	14	1.06	.	.	.	.	.	.
33	7N	30	1.28	0.28	81	0.61	0.01	303	0.00
34	7N	60	1.22	0.62	70	0.75	0.02	465	0.22
35	7N	90	0.42	0.50	87	0.44	4.19	313	0.82
36	8N	0	0.00	0.34	45	0.79	0.02	506	0.10
37	8N	14	0.78	.	.	.	.	.	.
38	8N	30	0.84	0.81	80	0.75	0.03	553	0.76
39	8N	60	0.79	0.82	68	0.90	0.01	752	0.63
40	8N	90	0.41	0.00	92	0.18	4.12	895	0.14

(Continued)

[1] %, mass/volume of solution, or gm/100 ml of solution.
[2] ppm

Table 8. (Concluded)

OBS	COND	AGE	Ca	Mg	Fe	S	Cl	Al	Na
1	1S	0	0.00	17.13	868	2.32	53.91	464	14.26
2	1S	14	0.35	.	.	.	.	.	.
3	1S	30	0.42	15.50	59	0.98	52.17	354	13.37
4	1S	60	1.60	17.70	148	1.58	52.22	442	13.02
5	1S	90	0.84	10.75	69	0.77	51.53	395	11.48
6	2S	0	0.01	12.69	1500	0.55	52.54	370	8.56
7	2S	14	0.91	.	.	.	.	.	.
8	2S	30	1.24	16.92	639	0.57	52.07	367	11.57
9	2S	60	2.00	21.04	810	0.64	52.26	415	11.81
10	2S	90	2.63	12.42	157	0.64	53.35	709	11.63
11	3S	0	0.00	2.30	52	2.39	65.47	796	43.65
12	3S	14	0.44	.	.	.	.	.	.
13	3S	30	0.33	4.74	58	1.68	60.81	113	31.67
14	3S	60	0.37	9.80	62	1.92	62.18	430	36.70
15	3S	90	0.10	2.56	32	2.11	64.47	718	41.00
16	4S	0	0.00	3.20	556	0.99	9.52	365	2.86
17	4S	14	1.98	.	.	.	.	.	.
18	4S	30	2.74	1.99	139	0.54	10.45	570	3.56
19	4S	60	3.54	0.07	225	0.70	10.80	677	3.57
20	4S	90	2.18	0.48	96	0.44	12.67	239	2.26
21	5S	0	0.00	0.53	42	0.88	66.10	377	36.13
22	5S	14	0.40	.	.	.	.	.	.
23	5S	30	0.38	7.60	108	0.59	62.49	363	30.11
24	5S	60	0.57	10.13	64	0.85	64.40	661	35.15
25	5S	90	0.15	2.23	40	0.69	65.17	781	36.54
26	6S	0	0.01	1.10	52	5.85	2.30	664	4.15
27	6S	14	0.64	.	.	.	.	.	.
28	6S	30	0.65	8.86	65	3.69	4.71	348	4.91
29	6S	60	1.83	8.47	61	3.61	4.32	385	4.83
30	6S	90	0.30	1.13	58	2.67	9.37	490	5.22
31	7S	0	0.09	0.63	78	0.91	0.01	814	0.29
32	7S	14	1.18	.	.	.	.	.	.
33	7S	30	1.26	0.71	119	0.49	2.35	410	1.45
34	7S	60	1.54	0.65	106	0.47	2.24	353	1.35
35	7S	90	0.43	0.00	84	0.19	5.60	896	0.24
36	8S	0	0.00	0.34	45	0.79	0.02	506	0.10
37	8S	14	.	.	.	.	.	.	.
38	8S	30	0.75	0.00	92	0.39	2.05	262	0.00
39	8S	60	0.75	0.68	75	0.65	1.94	477	1.38
40	8S	90	0.50	0.30	47	0.39	5.18	.	0.65

Calcium and chloride were the only ions that showed any measurable tendency to come out of the paste. Ca ion levels increased significantly in solution 2 (high Mg, low sulfate, high Cl) and 4 (moderate Mg), but were only slightly elevated in solution 1 (high Mg, high sulfate, high Cl). Chloride ion levels were elevated when salt-containing specimens were exposed to solutions 6, 7, and 8. High chloride ion levels at 90 days are due to the addition of HCl to acidify the solutions.

There was a pattern for some solutions to show higher calcium and magnesium levels at 14, 30, and 60 days than at 90 days. This is believed to be an artifact of the acid treatment at 90 days. Solutions that had not been acidified tended to be cloudy with suspended insoluble materials. It seems probable that during analysis, these phases settled onto the bottom window of the XRF sample container, thus getting preferential exposure to the incident X-rays. This caused the suspended phases to be over-represented in the analysis up to 60 days. At 90 days, acidification caused dissolution of these phases before the post-test solutions were analyzed. Therefore, 90-day data probably more accurately represent the total concentration of dissolved and particulate Mg and Ca compounds.

Mg ion levels showed no evidence of serious depletion in the high-Mg solutions (1 & 2), but there was measurable depletion in solution 4 by 90 days. This occurred in solutions containing both salt and non-salt specimens.

INTEGRATION OF RESULTS

Relationships Between Ca^{2+} Movement and Other Ions in Solution

The Ca loss detected by chemical analysis of discs exposed to high Mg concentrations corresponds with the disappearance of calcium hydroxide (CH), as determined by XRD (Table 5). However, Ca loss continued through 90 days, whereas CH was no longer detectable by 60 days. This indicates that a substantial amount of Ca must have been lost from other phases in the hydrated pastes in addition to that lost from calcium hydroxide.

In Figures 1 and 2, loss rates for all low-Mg solutions group together at the top of each Figure. Loss rates are similar for solutions 1, 2, and 4, with high and moderate Mg, at 30 days age. At later ages these curves diverge, with Ca loss from pastes appearing to continue at a faster rate in solutions with the highest Mg (curves 1 and 2, Figures 1 and 2). The rate of Ca loss also correlated with the concentration of Mg ion in the exposure solutions. If the early Ca losses are principally due to loss of CH, then this part of the reaction mechanism occurs whether the Mg concentration is moderate or high. There is an order of magnitude difference in the Mg concentration of the high-Mg solutions compared to the moderate-Mg solutions (Table 1).

Comparison of Ca lost with Mg gained by the specimens indicated that there was not a simple replacement of Ca by Mg in the pastes. The mechanism proposed earlier in this report indicates a Ca-to-Mg ratio of 1 in the first phase of the deterioration reaction (i.e., replacement of CH by MH), and a ratio of less than 1 in the second phase (i.e., formation of MSH). The changes in molar ratios of Ca to Mg in the paste at any time in the experiment relative to the controls were heavily skewed to values above one. Mg accumulation was not substantial until well after large amounts of Ca were lost from the paste. Figure 9 shows a high ratio of Ca loss relative to Mg gain at early ages. This ratio decreases with time, as Mg gain increases. Although Mg accumulation increased markedly by 90 days, molar ratios were still considerably above one.

There was no strong relationship between Ca movement from the hydrated paste and abundance of any component of the exposure solution other than Mg. However, there was a weak pattern involving sulfate ion concentration. Comparing the two high-Mg solutions (1 and 2), the one low in

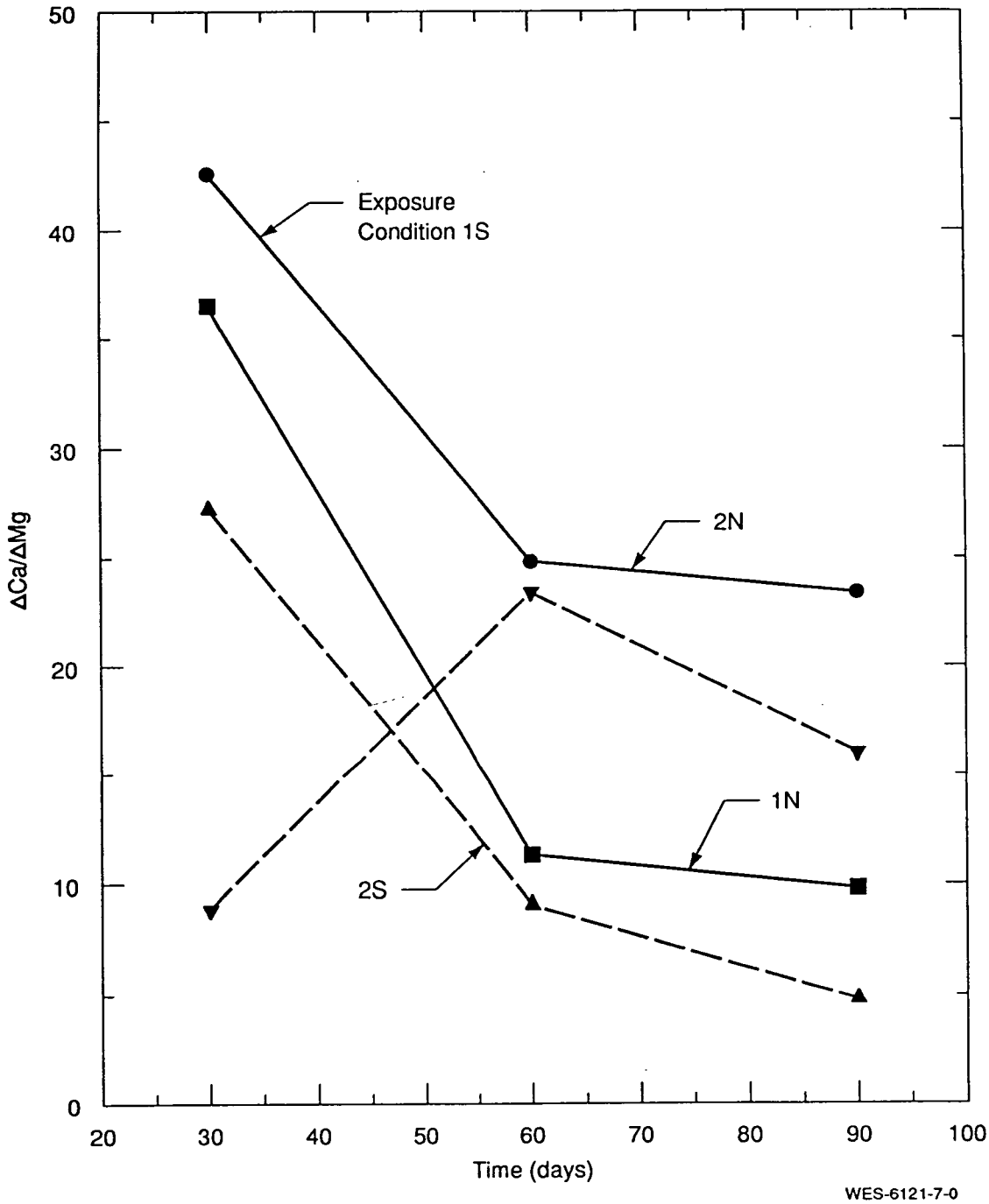

Figure 9. Molar ratio of Ca loss to Mg gain vs. exposure time.

sulfate (solution 2) appeared to be associated with a greater loss rate of Ca than was the solution high in sulfate (1). The difference was small, given the levels of experimental error associated with this work, but the pattern duplicated almost identically in both the salted and non-salted specimens.

There is no step in the published proposed mechanism of Mg attack suggesting that the presence of SO_4 should diminish the effect of Mg ion on Ca loss. To the contrary, it was expected that, if there was an effect, it would be to enhance Ca loss through the opening of the paste microstructure that sometimes occurs when calcium sulfoaluminate forms. The apparent reduced Ca loss in high SO_4 conditions could be attributable to the formation of gypsum from reaction of sulfate and calcium ions. Gypsum is a slightly soluble salt. Gypsum was detectable in the pastes exposed to high SO_4 environment of solution 1.

Levels of Cl and SO_4 in the exposure solution strongly affected the form taken by the released Ca. For example, the Ca lost during exposure to solution 1, which was highly concentrated in Mg, Cl, and SO_4, contributed to gypsum that crystallized on the surface of the specimen. Ca levels in solution did not increase much, evidently because most of the Ca stopped in this surface layer. In contrast, after exposure to solution 2, which differed from solution 1 in that SO_4 was low, the Ca concentration of the solution increased, and no Ca phases appeared on the surface of the specimen.

Relationships Between Cl^- and $SO_4^=$

Although Cl and SO_4 ions did not appear to have much affect on Ca loss from the hydrated cement system, these ions apparently were mobile. They reacted to form phases in the cement paste. When Cl ion concentrations were high in solution and initially low in the paste, they moved into the paste and reached equilibrium levels by the earliest test age, 30 days. When the reverse was true, the Cl ions moved out of the paste, again reaching approximate equilibrium by 30 days. High Cl-ion levels in the paste were associated with the formation of both halite and calcium chloroaluminate (CCA), but these compounds were not stable enough to hold the Cl there against the strong concentration gradient presented by low-Cl solutions.

As with Cl, SO_4 ions appeared to move readily into pastes when they were in high concentration in solution. When Cl concentrations in the pastes were low initially, i.e. non-salt specimens, the SO_4 formed calcium sulfoaluminate. Subsequent ingress of Cl did not appear to affect

this phase. When Cl concentrations in the pastes were high initially, i.e. salt specimens, calcium chloroaluminate formed and subsequent ingress of SO_4 resulted in the formation of gypsum. Ettringite formed only if the Cl concentration in brine was low, so that all Cl-bearing phases were leached out, allowing the sulfate to react with the aluminate phases. An example is seen in the salt specimens exposed to solution 6, which was highly concentrated in SO_4, but low in Cl and Mg. The Cl was leached out and SO_4 was incorporated in the discs, forming first gypsum (by 14 days), then ettringite (by 30 days; Table 5).

DISCUSSION

Mechanism of Deterioration

From previously published hypotheses of the mechanism of deterioration as discussed in the "Background" Chapter of this report, it was expected that Ca loss would be controlled by the action of Mg ion and that the replacement of Ca by Mg would be about 1:1 on a molar basis, at least initially. The results of this work support the hypothesis that the presence of Mg in an exposure solution promotes Ca depletion from hydrated paste. However, the rate of accumulation of Mg documented in this study does not indicate a simple one-for-one molar replacement, as would occur via the previously published mechanism.

A direct replacement of Ca by Mg may not be expected if the MSH is forming in large quantities and it has a different bonding relationship with Si. There is some unpublished evidence to suggest that the Mg-Si ratio in MSH is lower than the Ca-Si ratio in CSH. If this difference in ratios is real, and if large amounts of MSH had formed, then the apparent imbalance between Mg and Ca could be explained. However, there is no evidence in these data to indicate even the formation of MSH, although it is difficult to detect by the analytical methods used. Even if some MSH is forming, the ratios Ca lost to Mg gained in the pastes probably are too large to be explained by this difference in silicate bonding between CSH and MSH.

A notable amount of $Mg(OH)_2$ accumulated on the surfaces of the specimens that lost much Ca. We do not have total chemical analyses of these precipitates, so it is not possible to look at Ca-Mg ratios that include this source of Mg. However, the observed patterns suggest that Mg does not remove Ca at the site in the cement paste where the Ca exists. It may act more remotely, perhaps in a through-solution mechanism.

The Ca in the paste exists in two pools: in solution, and in solid phases such as CSH and $Ca(OH)_2$. The balance is far in favor of the solid phases. These two pools of Ca are in equilibrium through the liquid phase, so Ca exchange occurs between them. Ca loss from both pools could be explained as follows. The Ca in solution could move to the surface of the specimen, react there with Mg, and leave a Mg compound as Ca is released into the solution. Removal of the solubilized form of Ca causes more of the crystalline Ca compounds to go into solution, so the removal ultimately involves Ca from both pools.

As Ca is depleted from the near-surface regions of the specimen, the paste structure becomes more open and the pH decreases.. This allows Mg^{2+} to diffuse readily toward the interior of the sample establishing a new "front" for further removal of Ca.

$$Ca(OH)_2[solid] \rightharpoonup Ca^{2+} + 2OH^{1-} + Mg^{2+}[solution] \rightharpoonup Mg(OH)_2 + Ca^{2+}$$

This mechanism of reaction implies differences in the relative mobility of Ca^{2+} and OH^- ions, compared to that of Mg^{2+} and Cl^- ions. If the Ca and OH were more mobile, this would explain why they would move to the surface of the specimen and there react with Mg and Cl, rather than Mg and Cl moving into the specimen and reacting in place on the Ca compounds. If mobilities were about equal, or if Mg and Cl were more mobile in the cement paste, then it would be expected that the reaction would occur in the paste rather than at the surface of the specimen.

Although there are other controlling factors, the rate of diffusion of an ion should be related in some way to the effective radius of that ion. Ions tend to react electrically with water molecules, increasing their effective radius in aqueous solutions over the actual ionic radius. The hydrated radii of Cl^- and OH^- ions are similar: 30 nm for the former and 35 nm for the latter. The hydrated radius of Mg^{2+}, at 8 nm, is somewhat larger than the hydrated radius of Ca^{2+}, at 6 nm, even though Ca is larger than Mg. These relationships are consistent with the proposed hypothesis, but they probably represent a serious oversimplification. They require the assumption that cement paste is a highly porous medium to which conventional diffusion equations apply. Cement pastes are microporous at best, and many of the ions of interest here react with solid phases. Also, charges on solid-phase surfaces are likely to play an important role (Chatterji and Kawamura, 1992).

An unresolved question in this investigation is the lack of identity for the Mg compounds formed by the Mg that does accumulate in the pastes. MgO levels as high as 3.5% above controls accumulated in at least one paste, but no detectable Mg compounds were identified by XRD. According to the hypothesized deterioration mechanism, it was expected that either MH or MSH would be seen. MH is readily identifiable by XRD. If very much were present, it would have been detected. The diffraction pattern for MSH, on the other hand, is poorly described. There is at least one citation that indicates that MSH forms considerably after CSH is destroyed (Bonen, 1992), so perhaps its absence here is reasonable. It is notable that the exposure condition that resulted in the greatest Ca loss, solution 2S, also resulted in the greatest Mg gain.

Durability Implications

For the WIPP panel seals and other large concrete placements, the process of interest is the rate at which the concrete might lose structural integrity. Given that the strength-giving phases of cement-based concretes are Ca-containing compounds, it is reasonable to assume that degradation will be approximately proportional to the rate at which Ca is lost from the paste fraction of the concrete. There are other factors of this system that are important to long-term durability, as discussed below.

Ca is an essential component of several cementitious phases in concrete. CSH is generally considered to be the most abundant and most important. Either loss of this phase or replacement of it with MSH results in large strength loss of the paste. Calcium aluminate hydrates are important in determining setting behavior and early strength, but loss of these phases is not as critical for long-term strength.

Calcium hydroxide constitutes up to about 15% of hydrated cement paste (Lea, 1971). CH generally is more porous than CSH, and is thought to be more susceptible to chemical degradation processes than is CSH. Potentially more important, however, is the role of CH in bonding at the paste-aggregate interface. Most concretes have an interfacial zone of CH, surrounding all aggregate particles and providing much of the bond between hydrated cement pastes and aggregates.

The strength of the paste-aggregate interface is very important in determining strength of concrete, because this zone provides the bond between cement paste and aggregates (Bentz et al., 1992). If this phase were preferentially removed, its loss could have implications for loss of concrete strength that exceed its compositional level in the paste. The present study did not explore this question, because the experimental matrix was designed to delineate chemical reactions between brines and cement phases, so there were no aggregates. Other parameters of mixture proportioning, especially water-cement ratio, also exert strong controls on pore structure and on the rate at which strongly ionic fluids are transmitted to and through concrete. Efforts to use rate of Ca loss to estimate deterioration in a real exposure scenario must deal with these complexities.

Understanding the seal system requires knowing how each component will react relative to each other component: not only strength gain and response to lithostatic load, but possible strength loss with time. If all concrete components of the seal system could be located where there is no brine, then acceptable service of an appropriately proportioned and placed concrete is certain. But the

presence of brine brings the potential for chemical deterioration, and the possibility that a concrete may not maintain the properties measured at an early age.

Component materials and proportions can be selected to improve the chances of long-term durability if you know what is the most likely problem. Identifying the potential mechanisms of deterioration of concrete in WIPP brine is a necessary step in selecting component materials with enhanced chemical resistance. The strict performance requirements of a waste repository will demand that chemical properties and projected performance of a material are verified before its use. The results of this study also will be used in establishing a chemical test protocol for concrete to be used at the WIPP.

Approaches to Determining Rate of Deterioration

Past work at WES on cement-based materials for use at the WIPP has indicated that magnesium-based deterioration of hydrated portland cement materials is likely where Mg-ion concentrations are high in the ground water. Although careful tailoring of the materials used as components of concrete can mitigate and possibly delay the deterioration (Wakeley et al., 1993), some degradation of structural integrity is likely over the long term, and its prevention is not guaranteed by conventional variations in materials. Therefore, it is essential to develop the capability to estimate the rate of loss of integrity under exposure conditions likely to be encountered at the WIPP.

Three approaches have merit: real-time exposures, accelerated-time exposures, and modeling based on estimates of deterioration of small volumes of material. These are discussed individually below.

The advantage of real-time exposure of relatively large-scale specimens to ground water is that it minimizes the number of assumptions that must be made about the system. There are several weaknesses. One is the extended time required to get enough deterioration to develop a reasonably quantitative evaluation. Exposure of 2-in. mortar cubes required about a year to give measurable results, and then the deterioration involved only the first few millimetres in from the surface of the specimen. Another weakness is that results apply only to the specific materials and conditions represented in the test, which taken with the problem of testing time creates a cumbersome evaluation procedure. Still another problem exists in developing suitable evaluation criteria. Deterioration of large specimens immersed in brine is not homogeneous throughout the specimen, but develops as a slow-moving zone of deterioration from the outside. Measuring compressive strength then indicates an average integrity of the specimen and is not sensitive to zoning or other details of the deterioration process. Measuring some property such as fundamental frequency could be used to indicate rate of deterioration, but it is difficult to interpret the implications of such a test directly to engineering properties and field performance.

Accelerated-time testing such as exposure to higher temperature is an improvement on real-time testing, in that it can reduce the effect of cumbersome time-related problems. However, scaling results to real time is difficult unless there is some extended real-time data with which to calibrate the accelerated test method.

Another approach is to measure real-time rate of deterioration on a specimen small enough that significant effects can be observed in a short time. These effects then can be extrapolated to a larger mass of concrete through a mathematical model. If the specimen is small enough, then changes at a specific time can be considered to be homogeneous throughout. Consequently, evaluation criteria are more easily interpreted. The negative side of this approach is that assumptions are required about the way deterioration spreads, beyond the small unit volume in direct contact with the solution to other unit volumes located farther from the surface. The simplest assumption is one in which deterioration on the surface is linearly extrapolated into the specimen. This probably results in the worst-case scenario, but may be too simple. It is possible that deterioration on the surface of the concrete will retard the rate of deterioration of subsurface material.

This third approach has another advantage. Modeling allows the convenient exploration of many conditions, such as brine flow scenarios and Mg concentration profiles, without the encumbrance of real-time testing. Given the relatively rapid rate of reactions observed in this study, a combination of real-time testing and modelling is recommended.

Subsequent work at WES will explore the microstructure of concrete specimens before and after brine exposure. Results of this work are being analyzed to determine whether the loss of Ca ions occurs through general mass loss, or if it causes localized opening of the pore structure. Deterioration had progressed only about 1 mm into samples exposed to high-magnesium brine for 15 months. This work will be reported during 1994, and should provide another tool to use in determining implications for long-term integrity of concrete seals. These early results indicate that deterioration is very slow even where brine supply is unlimited and a large surface area is exposed.

CONCLUSIONS

Deterioration of portland cement pastes in brines containing high concentrations of Mg, Cl, and SO_4 is due principally to the reaction between the Mg in solution and the Ca in the hydrated cement. Other salts are less important in the relatively low-aluminate system investigated. The results support the hypothesis of deterioration by Ca loss in the presence of Mg. Calcium hydroxide was shown to be the principal source of Ca ions removed by this reaction, accompanied by softening of the paste. This loss is not accompanied by deposition of MH in the cement paste. But, MH accumulated on surfaces and as a suspended phase. More Ca leaves the cement paste than can be accounted for by the CH. Yet some CSH persisted. We found no evidence for formation of MSH, thought previously to be the principal phase that forms during Mg-related deterioration.

Accumulation of Mg in cement paste does not directly indicate deterioration. Consistently, far more Ca leaves than the amount of Mg that is added to the crystalline phase assemblage remaining as deteriorated cement paste. Because the strength of a concrete is attributed by Ca-bearing phases, Ca loss from the cementitious system should be a useful tool with which to investigate deterioration of candidate systems: knowing amount of Ca lost should permit calculation of loss of structural integrity. Determining which pools of Ca are most affected and how this relates to physical properties will provide an essential tool for establishing a standard chemical testing protocol for concretes to be used at the WIPP.

REFERENCES

Bentz, D.P., P.E. Stutzman, and E.J. Garboczi. 1992. "Experimental and Simulation Studies of the Interfacial Zone in Concrete," *Cement and Concrete Research*. Vol. 22, no. 5, 891-902.

Biczok, I.D. 1972. *Concrete Corrosion Concrete Protection*. 8th ed. Budapest: Akademiai Kiado.

Bonen, D. 1992. "Composition and Appearance of Magnesium Silicate Hydrate and Its Relation to Deterioration of Cement-Based Materials," *Journal of the American Ceramics Society*. Vol. 75, no. 10, 2904-2906.

Bonen, D., and M.D. Cohen. 1992. "Magnesium Sulfate Attack on Portland Cement Paste - I. Microstructural Analysis," *Cement and Concrete Research*. Vol. 22, no. 1, 169-180.

Buck, A.D., K. Mather, and B. Mather. 1984. *Cement Composition and Concrete Durability in Sea Water*. Technical Report SL-84-21. Vicksburg, MS: U.S. Army Engineer Waterways Experiment Station.

Chatterji, S., and M. Kawamura. 1992. "Electrical Double Layer, Ion Transport and Reactions in Hardened Cement Paste," *Cement and Concrete Research*. Vol. 22, no. 5, 774-782.

Ftikos, C., and G. Parissakis. 1985. "The Combined Action of Mg^{2+} and Cl^- Ions in Cement Pastes," *Cement and Concrete Research*. Vol. 15, no. 4, 593-599.

Gulick, C.W., and L.D. Wakeley. 1989. *Reference Properties of Cement-Based Plugging and Sealing Materials for the Waste Isolation Pilot Plant (WIPP)*. Technical Report SL-89-17. Vicksburg, MS: U.S. Army Engineer Waterways Experiment Station.

Harmon, J.C., G. Wyld, and T.C. Yao. 1978. "X-Ray Fluorescence Analysis of Stainless Steels and Low Alloy Steels Using Secondary Targets and the EXACT Program," *Advances in X-Ray Analysis, Proceedings of the Annual Conference on Applications of X-Ray Analysis, Denver, CO, August 1-4, 1978*. New York, NY: Plenum Press. 325-335.

Helmy, I.M., A.A. Amer, H. El-Didamony, and A.M. Amin. 1991. "Chemical Attack on Hardened Pastes of Blended Cements. Part I: Attack of Chloride Ions," *Zement-Kalk-Gipps*. Edition B. Vol. 44, no. 1, 46-50.

Kevex Instruments. 1990. *Kevex XRF Toolbox™ II Reference Manual*. P/N 7180-5060 C. Valencia CA: Kevex Instruments. (Copy on file at the Nuclear Waste Management Library, Sandia National Laboratories, Albuquerque, NM.)

Krumhansl, J.L., K.M. Kimball, and C.L. Stein. 1991. *Intergranular Fluid Compositions from the Waste Isolation Pilot Plant (WIPP), Southeastern New Mexico*. SAND90-0584. Albuquerque, NM: Sandia National Laboratories.

Kuenning, W.H. 1966. "Resistance of Portland Cement Mortar to Chemical Attack - A Progress Report," *Highway Research Record Number 113, Symposium on Effects of Aggressive Fluids on Concrete, 44th Annual Meeting, January 11-15, 1965*. Washington, DC: Highway Research Board of the Division of Engineering and Industrial Research, National Academy of Sciences-National Research Council. 43-87.

Lambert, S.J., E.J. Nowak, L.D. Wakeley, and T.S. Poole. 1992. "Interactions Between Concrete and Brine at the Waste Isolation Pilot Plant (WIPP) Site, New Mexico," *Scientific Basis for Nuclear Waste Management, Annual Fall Meeting of the Materials Research Society, Boston, MA, December 2-6, 1991.* Eds. F.P. Glasser, P.L. Pratt, T.O. Mason, J.F. Young, and G.J. McCarthy. SAND91-1421. Pittsburgh, PA: Materials Research Society. 111-116.

Lankard Materials Laboratory, Inc. 1991. *Final Report No. I-2480-3 on Deterioration of the Waste Shaft Liner Concrete at the WIPP Site to Westinghouse Electric Corporation, Waste Isolation Pilot Plant, Carlsbad, New Mexico.* Columbus, OH: Lankard Materials Laboratory, Inc. (Copy on file at the Nuclear Waste Management Library, Sandia National Laboratories, Albuquerque, NM.)

Lea, F.M. 1971. *The Chemistry of Cement and Concrete.* 3rd ed. New York, NY: Chemical Publishing Co.

Massazza, F. 1985. "Concrete Resistance to Seawater and Marine Environment," *Il Cimento.* Vol. 82, no. 1, 3-26.

Mather, B. 1966. "Effects of Seawater on Concrete," *Highway Research Record No. 113. Symposium on Effects of Aggressive Fluids on Concrete, 44th Annual Meeting, January 11-15, 1965.* Washington, DC: Highway Research Board of the Division of Engineering and Industrial Research, National Academy of Sciences-National Research Council. 33-42.

Oberste-Padtberg, R. 1985. "Degradation of Cements by Magnesium Brines," *Proceedings of the Seventh International Conference on Cement Microscopy.* Eds. J. Bayles, G.R. Gouda, and A. Nisperos. Duncanville, TX: International Cement Microscopy Association. 24-36.

Smith, D.K. 1990. *Cementing.* Richardson, TX: Society of Petroleum Engineers.

Smolczyk, H.G. [1968.] "Supplementary Paper III-31 Chemical Reactions of Strong Chloride-Solutions with Concrete," *Proceedings of the Fifth International Symposium on the Chemistry of Cement, Tokyo, 1968. Part III, Properties of Cement Paste and Concrete (Volume III).* The Cement Association of Japan. 274-280. (Copy on file at the Nuclear Waste Management Library, Sandia National Laboratories, Albuquerque, NM.)

Wakeley, L.D. 1990. "Grouts and Concretes for the Waste Pilot Project (WIPP)," *Scientific Basis for Nuclear Waste Management XIII, Materials Research Society Symposium Proceedings, Boston, MA, November 27-30, 1989.* Eds. V.M. Oversby and P.W. Brown. Pittsburgh, PA: Materials Research Society. Vol. 176, 45-51.

Wakeley, L.D., T.S. Poole, C.A. Weiss, [Jr.], and J.P. Burkes. [1992.] "Geochemical Stability of Cement-Based Composites in Magnesium Brines," [*Proceedings of the Fourteenth International Conference on Cement Microscopy.* Duncanville, TX: International Cement Microscopy Association. 333-342.] (Copy on file at the Nuclear Waste Management Library, Sandia National Laboratories, Albuquerque, NM.)

Wakeley, L.D., P.T. Harrington, and C.A. Weiss, Jr. 1993. *Properties of Salt-Saturated Concrete and Grout after Six Years In Situ at the Waste Isolation Pilot Plant.* SAND93-7019. Albuquerque, NM: Sandia National Laboratories.

APPENDIX A: PROPORTIONS OF SALADO MASS CONCRETE, AND PROPERTIES OF CEMENT AND STANDARD BRINE

Table A-1. Mixture Proportions, Salado Mass Concrete	
Mixture/Component	lb/yd^3
Cement, Class H, sulfate-resistant oil well cement	190
Class F Fly Ash	263
Fine Aggregate	1,294
Coarse Aggregate	1,658
Salt	84
Chem Comp	110
Na Citrate	3.5
Air Detraining Agent	5.6
Water	246

Table A-2. Chemical and Physical Description of Class H Oilwell Cement, HAN-1 C-1

Chemical Analysis		Physical Properties	
Property	Analysis (%)	Property	Analysis
SiO_2	22.4	Surface Area (Blaine)	235 m^2/kg
Al_2O_3	4.O		
Fe_2O_3	3.9	Autoclave	
CaO	64.0	Expansion	-0.03%
MgO	1.5		
SO_3	2.6	Initial Set (Gil)	155 min
Loss on Ignition	0.7	Final Set (Gil)	205 min
Insoluble Residue	0.26		
Na_2O	0.28	Air Content	9%
K_2O	0.63		
TiO_2	0.22	3-day Strength	1490 psi
P_2O_5	0.08	7-day Strength	2420 psi
C_3A	5		
C_3S	49		
C_2S	27		
C_4AF	12		

Table A-3. Composition of Brine Used as EDX Standard	
Component	Concentration (gm/100 ml)
NaCl, reagent grade	10.00
$MgCl_2.2H_2O$, reagent grade	19.37
$MgSO_4.7H_2O$, reagent grade	4.00
KCl, reagent grade	3.00
$CaCl_2.2H_2O$, reagent grade	0.73
Fe, 1000 ppm spectral standards	0.004 (40 ppm)
Al, 1000 ppm spectral standards	0.001 (10 ppm)
Si, 1000 ppm spectral standards	0.025 (250 ppm)

APPENDIX B: DESCRIPTION OF SURFACE DEPOSITS ON DISCS AFTER 60 DAYS EXPOSURE TIME

APPENDIX B: DESCRIPTION OF SURFACE DEPOSITS ON DISCS AFTER 60 DAYS EXPOSURE TIME

Five-digit sample designator is solution number, salt or non-salt (S or N), and age (days).

01N60: Disc was covered with thick white deposits, in clumps and patches of needle-like crystals.

01S60: Looked basically the same as 01N60 with fewer needles.

02N60: Thick, clear to white crystalline material covered the disc.

02S60: Looked the same as 02N60, but had less material on the disc.

03N60: The brine solution was cloudy, and the disc had white precipitate only on the outer rim with minimal clear crystalline precipitate on the rest of the surface.

03S60: The brine solution was cloudy, and the disc had a thin precipitate layer continuous over its surface.

04N60: A clear-to-white precipitate layer covered entire disc; precipitate on the bottom of the container.

04S60: Looked the same as 04N60.

05N60: The brine solution was cloudy. There was no precipitate on the disc, but there were small cubic crystals in patches on the surface.

05S60: Same as 05N60, but fewer patches.

06N60: The brine solution was cloudy. The whole disc was covered with small clear crystalline patches.

06S60: Brine solution was cloudy, and the disc had the same appearance as 06N60.

07N60: Clear brine, and no precipitate on the disc.

07S60: Same as 07N60.

APPENDIX C: UNCORRECTED AND Fe-CORRECTED CHEMICAL ANALYSIS OF DISCS

APPENDIX C: UNCORRECTED AND Fe-CORRECTED CHEMICAL ANALYSIS OF DISCS

Uncorrected										
					SAS		10:29 Tuesday, January 26, 1993 65			
OBS	COND	AGE	CaO	MgO	SiO_2	SO_4	Cl	AL_2O_3	Fe_2O_3	Na_2O
52	CS	30	56.0	1.31	19.6	2.29	7.57	3.50	3.42	4.92
53	CS	60	56.8	1.27	18.0	2.12	7.65	3.32	3.43	4.90
54	CS	90	56.8	1.23	18.1	2.39	9.00	3.30	3.32	6.84
4	1S	30	52.9	1.67	21.4	3.19	11.32	3.85	3.97	4.96
5	1S	60	50.8	2.13	23.0	3.41	10.64	4.53	4.65	2.08
6	1S	90	49.2	2.46	24.5	4.14	13.46	4.81	4.94	5.28
10	2S	30	52.9	1.89	22.1	2.96	12.06	4.00	4.09	5.41
11	2S	60	49.4	3.42	23.7	2.76	10.53	4.69	4.95	2.20
12	2S	90	45.1	7.61	27.5	3.04	12.55	5.58	5.10	4.15
16	3S	30	57.5	1.28	18.6	3.70	7.64	3.29	3.49	5.97
17	3S	60	57.6	1.34	18.6	3.36	7.39	3.47	3.70	5.72
18	3S	90	58.4	1.35	19.9	3.99	7.62	3.72	3.58	5.80
22	4S	30	57.6	1.64	24.4	5.39	3.93	4.29	4.17	0.86
23	4S	60	58.5	1.70	23.9	4.58	2.65	4.42	4.42	0.43
24	4S	90	58.5	1.76	26.0	5.52	5.52	4.94	4.42	0.44
28	5S	30	59.0	1.32	20.0	1.46	7.44	3.48	3.50	2.84
29	5S	60	57.5	1.23	18.9	0.90	6.92	3.49	3.72	2.67
30	5S	90	59.5	1.30	21.1	1.08	7.73	3.86	3.56	2.89
34	6S	30	59.6	1.34	20.8	7.14	1.13	3.51	3.56	0.91
35	6S	60	59.2	1.33	19.9	7.08	0.68	3.53	3.71	0.77
36	6S	90	61.2	1.43	22.2	8.43	0.70	3.97	3.75	1.43
40	7S	30	63.0	1.37	21.9	2.41	1.65	3.74	3.54	0.53
41	7S	60	62.5	1.37	21.2	2.23	1.31	3.80	3.68	0.15
42	7S	90	63.9	1.38	22.6	2.55	1.19	4.17	3.73	0.12
46	8S	30	62.0	1.32	20.4	2.29	1.66	3.53	3.69	0.39
47	8S	60	62.0	1.39	21.3	2.25	1.32	3.82	3.75	0.15
48	8S	90	64.5	1.58	24.7	2.75	1.49	4.60	3.78	0.33

Uncorrected										
OBS	COND	AGE	CaO	MgO	SiO_2	SO_4	Cl	Al_2O_3	Fe_2O_3	Na_2O
49	CN	30	61.6	1.43	20.9	2.49	0.07	3.91	3.61	0.26
50	CN	60	62.4	1.38	19.7	2.53	0.40	3.68	3.59	0.51
51	CN	90	63.2	1.50	22.5	2.74	0.05	4.42	3.61	0.33
1	1N	30	54.4	1.76	22.3	3.95	9.12	4.21	4.06	2.73
2	1N	60	53.0	2.47	22.7	4.31	9.82	4.49	4.41	2.00
3	1N	90	49.3	3.34	24.3	4.62	11.78	4.91	4.60	4.50
7	2N	30	55.4	2.14	21.4	3.28	8.36	4.39	4.10	2.37
8	2N	60	52.0	2.19	23.7	3.29	8.96	4.59	4.35	2.47
9	2N	90	50.5	3.14	26.8	3.66	10.21	5.34	4.53	2.08
13	3N	30	58.5	1.32	18.6	3.86	6.15	3.43	3.50	4.40
14	3N	60	58.7	1.43	18.7	4.49	6.03	3.60	3.50	4.22
15	3N	90	59.7	1.46	20.6	4.62	5.31	4.01	3.53	3.75
19	4N	30	57.7	1.78	24.1	5.13	2.49	4.63	4.63	0.48
20	4N	60	57.1	1.63	22.5	4.92	2.36	4.28	4.20	0.44
21	4N	90	58.4	1.81	26.1	5.74	1.84	5.17	4.50	0.37
25	5N	30	57.9	1.36	19.2	2.32	6.75	3.57	3.49	4.17
26	5N	60	57.8	1.36	19.2	2.08	6.21	3.59	3.48	2.72
27	5N	90	60.0	1.31	20.3	2.10	6.52	3.81	3.66	3.38
31	6N	30	61.1	1.55	20.3	5.94	0.35	3.75	3.55	0.42
32	6N	60	59.0	1.42	19.1	7.39	0.78	3.59	3.58	0.77
33	6N	90	61.5	1.45	21.5	8.99	0.25	4.17	3.62	0.56
37	7N	30	61.6	1.54	22.1	2.83	0.67	4.10	3.59	0.16
38	7N	60	62.1	1.52	20.9	2.56	0.19	4.14	3.65	0.17
39	7N	90	62.3	1.50	22.5	2.68	0.05	4.38	3.68	0.11
43	8N	30	63.7	1.51	21.7	2.73	0.06	4.05	3.72	0.11
44	8N	60	62.2	1.50	21.9	2.84	0.20	3.97	3.64	0.25
45	8N	90	63.6	1.60	24.1	2.80	0.05	4.74	3.77	0.18

CORRECTED BY Fe-RATIO METHOD										
OBS	COND	AGE	CaO	MgO	SiO_2	SO_4	Cl	Al_2O_3	Na_2O	CF
25	CS	30	55.51	1.30	19.43	2.27	7.50	3.47	4.88	0.991
26	CS	60	56.14	1.26	17.79	2.10	7.56	3.28	4.84	0.988
27	CS	90	58.00	1.26	18.48	2.44	9.19	3.37	6.98	1.021
1	1S	30	45.17	1.43	18.27	2.72	9.67	3.29	4.24	0.854
2	1S	60	37.03	1.55	16.77	2.49	7.76	3.30	1.52	0.729
3	1S	90	33.76	1.69	16.81	2.84	9.24	3.30	3.62	0.686
4	2S	30	43.85	1.57	18.32	2.45	10.00	3.32	4.48	0.829
5	2S	60	33.83	2.34	16.23	1.89	7.21	3.21	1.51	0.685
6	2S	90	29.98	5.06	18.28	2.02	8.34	3.71	2.76	0.665
7	3S	30	55.85	1.24	18.07	3.59	7.42	3.20	5.80	0.971
8	3S	60	52.77	1.23	17.04	3.08	6.77	3.18	5.24	0.916
9	3S	90	55.30	1.28	18.84	3.78	7.22	3.52	5.49	0.947
10	4S	30	46.83	1.33	19.84	4.38	3.19	3.49	0.70	0.813
11	4S	60	44.87	1.30	18.33	3.51	2.03	3.39	0.33	0.767
12	4S	90	44.87	1.35	19.94	4.23	4.23	3.79	0.34	0.767
13	5S	30	57.15	1.28	19.37	1.41	7.21	3.37	2.75	0.969
14	5S	60	52.40	1.12	17.22	0.82	6.31	3.18	2.43	0.911
15	5S	90	56.66	1.24	20.09	1.03	7.36	3.68	2.75	0.952
16	6S	30	56.75	1.28	19.81	6.80	1.08	3.34	0.87	0.952
17	6S	60	54.09	1.22	18.18	6.47	0.62	3.23	0.70	0.914
18	6S	90	55.32	1.29	20.07	7.62	0.63	3.59	1.29	0.904
19	7S	30	60.33	1.31	20.97	2.31	1.58	3.58	0.51	0.958
20	7S	60	57.57	1.26	19.53	2.05	1.21	3.50	0.14	0.921
21	7S	90	58.08	1.25	20.54	2.32	1.08	3.79	0.11	0.909
22	8S	30	56.96	1.21	18.74	2.10	1.53	3.24	0.36	0.919
23	8S	60	56.05	1.26	19.26	2.03	1.19	3.45	0.14	0.904
24	8S	90	57.85	1.42	22.15	2.47	1.34	4.13	0.30	0.897

OXIDE ANALYSIS CORRECTED BY Fe-RATIO METHOD										
OBS	COND	AGE	CaO	MgO	SiO_2	SO_4	Cl	Al_2O_3	Na_2O	CF
25	CN	30	61.43	1.43	20.84	2.48	0.07	1.90	0.26	0.997
26	CN	60	62.57	1.38	19.75	2.54	0.40	3.69	0.51	1.003
27	CN	90	63.02	1.50	22.44	2.73	0.05	4.41	0.33	0.997
1	1N	30	48.24	1.56	19.77	3.50	8.09	3.73	2.42	0.887
2	1N	60	43.27	2.02	18.53	3.52	8.02	3.67	1.63	0.816
3	1N	90	38.58	2.61	19.02	3.62	9.22	3.84	3.52	0.783
4	2N	30	48.64	1.88	18.79	2.88	7.34	3.85	2.08	0.878
5	2N	60	43.03	1.81	19.61	2.72	7.42	3.80	2.04	0.828
6	2N	90	40.13	2.50	21.30	2.91	8.11	4.24	1.65	0.795
7	3N	30	60.17	1.36	19.13	3.97	6.33	3.53	4.53	1.029
8	3N	60	60.38	1.47	19.23	4.62	6.20	3.70	4.34	1.029
9	3N	90	60.88	1.49	21.01	4.71	5.42	4.09	3.82	1.020
10	4N	30	44.86	1.38	18.74	3.99	1.94	3.60	0.37	0.778
11	4N	60	48.94	1.40	19.29	4.22	2.02	3.67	0.38	0.857
12	4N	90	46.72	1.45	20.88	4.59	1.47	4.14	0.30	0.800
13	5N	30	59.72	1.40	19.81	2.39	6.96	3.68	4.30	1.032
14	5N	60	59.79	1.41	19.86	2.15	6.42	3.71	2.81	1.034
15	5N	90	59.02	1.29	19.97	2.07	6.41	3.75	3.32	0.984
16	6N	30	61.96	1.57	20.59	6.02	0.35	3.80	0.43	1.014
17	6N	60	59.33	1.43	19.21	7.43	0.78	3.61	0.77	1.006
18	6N	90	61.16	1.44	21.38	8.94	0.25	4.15	0.56	0.994
19	7N	30	61.77	1.54	22.16	2.84	0.67	4.11	0.16	1.003
20	7N	60	61.25	1.50	20.61	2.52	0.19	4.08	0.17	0.986
21	7N	90	60.95	1.47	22.01	2.62	0.05	4.28	0.11	0.978
22	8N	30	61.65	1.46	21.00	2.64	0.06	3.92	0.11	0.968
23	8N	60	61.52	1.48	21.66	2.81	0.20	3.93	0.25	0.989
24	8N	90	60.73	1.53	23.01	2.67	0.05	4.53	0.17	0.955

DISTRIBUTION

Federal Agencies

US Department of Energy (6)
Office of Civilian Radioactive Waste Management
Attn: Deputy Director, RW-2
Associate Director, RW-10/50
Office of Program and Resources Management
Office of Contract Business Management
Director, RW-22
Analysis and Verification Division
Associate Director, RW-30
Office of Systems and Compliance
Associate Director, RW-40
Office of Storage and Transportation
Director, RW-4/5
Office of Strategic Planning and International Programs
Office of External Relations
Forrestal Building
Washington, DC 20585

US Department of Energy
Albuquerque Operations Office
Attn: National Atomic Museum Library
PO Box 5400
Albuquerque, NM 87185-5400

US Department of Energy (4)
WIPP Project Integration Office
Attn: W.J. Arthur III
L.W. Gage
P.J. Higgins
D.A. Olona
PO Box 5400
Albuquerque, NM 87115-5400

US Department of Energy (2)
WIPP Project Integration Satellite Office
Attn: R. Batra
R. Becker
PO Box 3090, Mail Stop 525
Carlsbad, NM 88221-3090

US Department of Energy
Research & Waste Management Division
Attn: Director
PO Box E
Oak Ridge, TN 37831

US Department of Energy (3)
WIPP Project Site Office (Carlsbad)
Attn: V. Daub
J. Lippis
J.A. Mewhinney
PO Box 3090
Carlsbad, NM 88221-3090

US Department of Energy
Attn: E. Young
Room E-178
GAO/RCED/GTN
Washington, DC 20545

US Department of Energy
Office of Environmental Restoration and Waste Management
Attn: J. Lytle, EM-30,
Trevion II
Washington, DC 20585-0002

US Department of Energy (3)
Office of Environmental Restoration and Waste Management
Attn: M. Frei, EM-34,
Trevion II
Washington, DC 20585-0002

US Department of Energy
Office of Environmental Restoration and Waste Management
Attn: S. Schneider, EM-342,
Trevion II
Washington, DC 20585-0002

US Department of Energy (2)
Office of Environment, Safety and Health
Attn: C. Borgstrom, EH-25
R. Pelletier, EH-231
Washington, DC 20585

US Department of Energy (2)
Idaho Operations Office
Fuel Processing and Waste Management Division
785 DOE Place
Idaho Falls, ID 83402

US Environmental Protection Agency (2)
Radiation Protection Programs
Attn: M. Oge
ANR-460
Washington, DC 20460

US Geological Survey (2)
Water Resources Division
Attn: R. Livingston
4501 Indian School NE
Suite 200
Albuquerque, NM 87110

US Nuclear Regulatory Commission
Division of Waste Management
Attn: H. Marson
Mail Stop 4-H-3
Washington, DC 20555

Boards

Defense Nuclear Facilities Safety Board
Attn: D. Winters
625 Indiana Ave. NW, Suite 700
Washington, DC 20004

Nuclear Waste Technical Review Board (2)
Attn: Chairman
S.J.S. Parry
1100 Wilson Blvd., Suite 910
Arlington, VA 22209-2297

Advisory Committee on Nuclear Waste
Nuclear Regulatory Commission
Attn: R. Major
7920 Norfolk Ave.
Bethesda, MD 20814

State Agencies

Environmental Evaluation Group (3)
Attn: Library
7007 Wyoming NE
Suite F-2
Albuquerque, NM 87109

NM Bureau of Mines and Mineral Resources
Socorro, NM 87801

NM Energy, Minerals, and Natural Resources Department
Attn: Library
2040 S. Pacheco
Santa Fe, NM 87505

NM Environment Department (3)
Secretary of the Environment
Attn: J. Espinosa
1190 St. Francis Drive
Santa Fe, NM 87503-0968

NM Environment Department
WIPP Project Site
Attn: P. McCasland
PO Box 3090
Carlsbad, NM 88221

Laboratories/Corporations

Battelle Pacific Northwest Laboratories
Attn: R.E. Westerman
MSIN P8-44
Battelle Blvd.
Richland, WA 99352

INTERA, Inc.
Attn: G.A. Freeze
1650 University NE, Suite 300
Albuquerque, NM 87102

INTERA, Inc.
Attn: J.F. Pickens
6850 Austin Center Blvd., Suite 300
Austin, TX 78731

INTERA, Inc.
Attn: W. Stensrud
PO Box 2123
Carlsbad, NM 88221

IT Corporation
Attn: R.F. McKinney
Regional Office
5301 Central NE, Suite 700
Albuquerque, NM 87108

Los Alamos National Laboratory
Attn: B. Erdal, INC-12
PO Box 1663
Los Alamos, NM 87544

RE/SPEC, Inc.
Attn: W. Coons
4775 Indian School NE, Suite 300
Albuquerque, NM 87110-3927

RE/SPEC, Inc.
Attn: J.L. Ratigan
PO Box 725
Rapid City, SD 57709

Southwest Research Institute (2)
Center for Nuclear Waste Regulatory Analysis
Attn: P.K. Nair
6220 Culebra Road
San Antonio, TX 78228-0510

SAIC
Attn: H.R. Pratt
10260 Campus Point Dr.
San Diego, CA 92121

SAIC (2)
Attn: M. Davis
J. Tollison
2109 Air Park Rd. SE
Albuquerque, NM 87106

Tech Reps Inc. (3)
Attn: J. Chapman
C. Crawford
T. Peterson
5000 Marble NE, Suite 222
Albuquerque, NM 87110

TRW Environmental Safety Systems
Attn: L. Wildman
2650 Park Tower Dr., Suite 1300
Vienna, VA 22180-7306

Waterways Experiment Station (2)
Attn: L.D. Wakeley
3909 Halls Ferry Rd.
Vicksburg, MS 39180-5927

Westinghouse Electric Corporation (5)
Attn: Library
C. Cox
L. Fitch
B.A. Howard
R. Kehrman
PO Box 2078
Carlsbad, NM 88221

Westinghouse–Savannah River
Technology Center (4)
Attn: N. Bibler
J.R. Harbour
M.J. Plodinec
G.G. Wicks
Aiken, SC 29802

National Academy of Sciences, WIPP Panel

Howard Adler
Oak Ridge Associated Universities
Medical Sciences Division
PO Box 117
Oak Ridge, TN 37831-0117

Ina Alterman
Board on Radioactive Waste
Management, GF456
2101 Constitution Ave.
Washington, DC 20418

Fred M. Ernsberger
1325 NW Tenth Ave.
Gainsville, FL 32605

John D. Bredehoeft
Western Region Hydrologist
Water Resources Division
US Geological Survey (M/S 439)
345 Middlefield Road
Menlo Park, CA 94025

Rodney C. Ewing
Department of Geology
University of New Mexico
Albuquerque, NM 87131

Charles Fairhurst
Department of Civil and Mineral
Engineering
University of Minnesota
500 Pillsbury Dr. SE
Minneapolis, MN 55455-0220

B. John Garrick
PLG Incorporated
4590 MacArthur Blvd., Suite 400
Newport Beach, CA 92660-2027

Leonard F. Konikow
US Geological Survey
431 National Center
Reston, VA 22092

Carl A. Anderson, Director
Board on Radioactive Waste Management
National Research Council
HA 456
2101 Constitution Ave. NW
Washington, DC 20418

Jeremiah O'Driscoll
Jody Incorporated
505 Valley Hill Drive
Atlanta, GA 30350

Christopher G. Whipple
ICF Kaiser Engineers
1800 Harrison St., 7th Floor
Oakland, CA 94612-3430

Individuals

P. Drez
8816 Cherry Hills Rd. NE
Albuquerque, NM 87111

K. Lickliter
400-C 8th St. SW
Tacoma, WA 98439

D.W. Powers
Star Route Box 87
Anthony, TX 79821

Universities

University of Missouri-Rolla
Department of Nuclear Engineering
Attn: N. Tsoulfanidis
102 Fulton Hall
Rolla, MO 65401-0249

University of New Mexico
Geology Department
Attn: Library
141 Northrop Hall
Albuquerque, NM 87131

University of Washington
College of Ocean & Fishery Sciences
Attn: G.R. Heath
583 Henderson Hall HN-15
Seattle, WA 98195

Libraries

Thomas Brannigan Library
Attn: D. Dresp
106 W. Hadley St.
Las Cruces, NM 88001

Government Publications Department
Zimmerman Library
University of New Mexico
Albuquerque, NM 87131

New Mexico Junior College
Pannell Library
Attn: R. Hill
Lovington Highway
Hobbs, NM 88240

New Mexico State Library
Attn: N. McCallan
325 Don Gaspar
Santa Fe, NM 87503

New Mexico Tech
Martin Speere Memorial Library
Campus Street
Socorro, NM 87810

WIPP Public Reading Room
Carlsbad Public Library
101 S. Halagueno St.
Carlsbad, NM 88220

Foreign Addresses

Studiecentrum Voor Kernenergie
Centre d'Énergie Nucléaire
Attn: A. Bonne
SCK/CEN Boeretang 200
B-2400 Mol, BELGIUM

Atomic Energy of Canada, Ltd. (3)
Whiteshell Laboratories
Attn: B. Goodwin
M. Stevens
D. Wushke
Pinawa, Manitoba, CANADA ROE 1LO

Francois Chenevier (2)
ANDRA
Route du Panorama Robert Schumann
B.P. 38
92266 Fontenay-aux-Roses, Cedex
FRANCE

Jean-Pierre Olivier
OECD Nuclear Energy Agency
Division of Radiation Protection and
Waste Management
38, Boulevard Suchet
75016 Paris, FRANCE

Claude Sombret
Centre d'Études Nucléaires de la
Vallee Rhone CEN/VALRHO
S.D.H.A. B.P. 171
30205 Bagnols-Sur-Ceze, FRANCE

Commissariat a L'Energie Atomique
Attn: D. Alexandre
Centre d'Études de Cadarache
13108 Saint Paul Lez Durance Cedex
FRANCE

Bundesanstalt für Geowissenschaften
und Rohstoffe
Attn: M. Langer
Postfach 510 153
D-30631 Hannover, GERMANY

Bundesministerium für Forschung und
Technologie
Postfach 200 706
5300 Bonn 2, GERMANY

Institut für Tieflagerung (2)
Attn: K. Kuhn
Theodor-Heuss-Strasse 4
D-3300 Braunschweig, GERMANY

Gesellschaft für Anlagen und
Reaktorsicherheit (GRS) (2)
Attn: B. Baltes
W. Muller
Schwertnergasse 1
D-50667 Cologne, GERMANY

Physikalisch-Technische Bundesanstalt
Attn: P. Brenneke
Postfach 3345
D-3300 Braunschweig, GERMANY

Shingo Tashiro
Japan Atomic Energy Research Inst.
Tokai-Mura, Ibaraki-Ken, 319-11
JAPAN

Netherlands Energy Research
Foundation ECN
Attn: L.H. Vons
3 Westerduinweg
PO Box 1
1755 ZG Petten
THE NETHERLANDS

Svensk Kärnbränsleforsorjning AB
Attn: F. Karlsson
Project KBS (Kärnbränslesakerhet)
Box 5864
S-102 48 Stockholm
SWEDEN

Nationale Genossenschaft für die
Lagerung radioaktiver Abfälle (2)
Attn: S. Vomvoris
P. Zuidema
Hardstrasse 73
CH-5430 Wettingen
SWITZERLAND

AEA Technology
Attn: J.H. Rees
D5W/29 Culham Laboratory
Abington, Oxfordshire OX14 3DB
UNITED KINGDOM

AEA Technology
Attn: W.R. Rodwell
044/A31 Winfrith Technical Centre
Dorchester, Dorset DT2 8DH
UNITED KINGDOM

AEA Technology
Attn: J.E. Tinson
B4244 Harwell Laboratory
Didcot, Oxfordshire OX11 0RA
UNITED KINGDOM

D.R. Knowles
British Nuclear Fuels, plc
Risley, Warrington, Cheshire WA3 6AS
1002607 UNITED KINGDOM

Internal

MS	Org.	
0827	1502	P.J. Hommert
0127	4511	D.P. Garber
0724	6000	D.L. Hartley
1324	6115	P.B. Davies
1324	6115	Staff (15)
0750	6118	J.L. Krumhansl
7050	6118	S.J. Lambert
1320	6119	E.J. Nowak
1320	6119	Staff (7)
1332	6121	J.R. Tillerson
1332	6121	Staff (7)
1335	6303	S.Y. Pickering
1335	6303	W.D. Weart
1335	6305	S.A. Goldstein
1335	6305	A.R. Lappin
1341	6306	A.L. Stevens
1328	6342	D.R. Anderson
1328	6342	Staff (20)
1395	6343	V.H. Slaboszewicz
1395	6343	Staff (2)
1341	6345	R.C. Lincoln
1341	6345	Staff (9)
1341	6347	D.R. Schafer
1341	6348	J.T. Holmes
1341	6348	Staff (4)
1343	6351	R.E. Thompson
1330	6352	G.M. Gerstner-Miller
1330	6352	WIPP Central Files (10)
0899	7141	Technical Library (5)
0619	7151	Technical Publications
0100	7613-2	Document Processing for DOE/OSTI (10)
9018	8523-2	Central Technical Files

U.S. Government Printing Office 1994-573-110-02070